NAVAL SHIP RESEARCH AND DEVELOPMENT CENTER
Washington, D.C. 20007

FLUTTER AND CAVITY-INDUCED OSCILLATION OF A TWO-DEGREE-OF-FREEDOM HYDROFOIL IN TWO-DIMENSIONAL CAVITATING FLOW

HYDROMECHANICS LABORATORY

RESEARCH AND DEVELOPMENT REPORT

April 1969

Report 3000

FLUTTER AND CAVITY-INDUCED OSCILLATION OF A TWO-DEGREE-OF-FREEDOM HYDROFOIL IN TWO-DIMENSIONAL CAVITATING FLOW

The Naval Ship Research and Development Center is a U.S. Navy center for laboratory effort directed at achieving improved sea and air vehicles. It was formed in March 1967 by merging the David Taylor Model Basin at Carderock, Maryland and the Marine Engineering Laboratory at Annapolis, Maryland. The Mine Defense Laboratory, Panama City, Florida became part of the Center in November 1967.

Naval Ship Research and Development Center
Washington, D.C. 20007

DEPARTMENT OF THE NAVY
NAVAL SHIP RESEARCH AND DEVELOPMENT CENTER
WASHINGTON, D. C. 20007

FLUTTER AND CAVITY-INDUCED OSCILLATION OF A TWO-DEGREE-OF-FREEDOM HYDROFOIL IN TWO-DIMENSIONAL CAVITATING FLOW

by

Peter K. Besch

April 1969 Report 3000

TABLE OF CONTENTS

LIST OF FIGURES

LIST OF TABLES

NOTATION

a	Distance of pitch axis from midchord of hydrofoil model, in units of semichord (positive aft)
b	Semichord of hydrofoil model
C_p	Pressure coefficient; $2(p-p_\infty)/\rho U^2$
E	Distance of cavity separation point aft of leading edge of hydrofoil, in chords
f	Frequency in Hertz
f_h	Natural frequency of uncoupled heave oscillation in air; theoretically $\sqrt{K_h/(m_h + m_\alpha)}$
f_α	Natural frequency of uncoupled pitch oscillation in air; theoretically $\sqrt{K_\alpha/I_\alpha}$
h	Vertical displacement of pitch axis from equilibrium position (positive downward)
I_α	Second moment of inertia of rotating mass about pitch axis
K_h	Heave spring stiffness
K_α	Pitch spring stiffness
L	Lift; positive upward
m_h	Mass of hydrofoil model and suspension which only translates
m_α	Mass of hydrofoil model and suspension which both rotates and translates
M	Pitching moment; positive when acting to increase angle of attack
p	Pressure
p_c	Pressure inside cavity
p_v	Water vapor pressure
p_∞	Static pressure
r_α	Radius of gyration of rotating mass, in units of semichord; $\sqrt{I_\alpha/m_\alpha}\ /b$
s	Span of hydrofoil model
S_α	First moment of inertia of rotating mass about pitch axis
U	Water speed
x_α	Distance of center of gravity from pitch axis, in units of semichord (positive aft); $S_\alpha/m_\alpha b$

α	Angle of attack relative to lower surface of hydrofoil model; refers to rotational mode when used as a subscript
β	Ratio of rotating mass to total mass of system; $m_\alpha/(m_h + m_\alpha)$
μ	Mass ratio of system; $(m_\alpha + m_h)/\pi\rho b^2 s$
ρ	Mass of water per unit volume
σ_c	Cavitation number based on cavity pressure; $2(p_\infty - p_c)/\rho U^2$
σ_v	Cavitation number based on water vapor pressure; $2(p_\infty - p_v)/\rho U^2$
ω	$2\pi f$
ω_h	$2\pi f_h$
ω_α	$2\pi f_\alpha$

ABSTRACT

Two hydrofoil flutter tests were performed at the Naval Ship Research and Development Center using a two-degree-of-freedom, semiwedge hydrofoil in two-dimensional cavitating flow. In the first test, conducted in the high-speed towing basin, four distinct cavity lengths were tested. Flutter occurred for cavities 1/2 and several chords in length. Cavity-induced oscillations may have occurred for 1-chord cavities, but no oscillations were observed for 2-chord cavities. The flutter results are compared with flutter boundaries predicted by partially cavitating and supercavitating flutter theories. It is concluded that the experimental flutter results do not disagree with the predicted values.

In the second test, conducted in the 24-in. variable-pressure water tunnel, cavity lengths were varied from 0 to 3 chords. Cavity-induced oscillations were observed for cavities between 0.4 and 1.4 chords in length, but other cavity lengths were free of oscillation. The oscillations are discussed in terms of forced oscillations of a coupled two-degree-of-freedom elastic system. It is concluded that the cavity-induced oscillations, unlike flutter, are positively damped oscillations. Several recommendations are given for further experimental and theoretical studies.

ADMINISTRATIVE INFORMATION

This work was performed as part of the Hydrofoil Accelerated Research Program and funded under Project S4606, Task 1703.

INTRODUCTION

Flutter is the dynamic instability of a wing-like structure caused by the interaction of fluid and elastic forces acting on the structure. On conventional marine vehicles such as ships and submarines, flutter might involve the various control surfaces which resemble low-aspect-ratio wings. This type of flutter, or a flutter-related vibration, may have occurred on the USS FORREST SHERMAN (DD-931), according to an analysis given by McGoldrick.[1] Subsequent tests performed by Jewell and McCormick[2] at the David Taylor Model Basin have shown that flutter can occur for hydroelastic

---

[1]References are listed on page 51.

parameters corresponding to typical rudder installations. In addition to ship control surfaces, the struts and foils used on high-speed hydrofoil craft now being introduced may be susceptible to flutter. With higher speeds being contemplated for all types of naval craft, accurate prediction of hydroelastic stability characteristics has become increasingly important.

A large body of successful flutter prediction methods has been developed for application to aircraft. It would clearly be desirable to employ existing airfoil flutter theories for predicting the flutter characteristics of hydrofoils. Subcavitating hydrofoils differ from airfoils only in the magnitude of certain parameters (mass ratio and reduced frequency) relating flow characteristics to structural properties. All parameters are readily accounted for in theory. Therefore airfoil flutter theories can be applied to fully wetted hydrofoils.

Several hydrofoil flutter experiments are available to provide a basis for comparison with airfoil theories. These theories have failed to predict the experimental results except where significant aspects of the calculation have been arbitrarily varied. However, no such variation has had successful general application to hydrofoil flutter. For example, swept, surface-piercing hydrofoils that were flutter tested by Baird et al.[3] were successfully treated by modal analysis only for a particular number of modes.[4,5] An unswept, fully submerged hydrofoil that was flutter tested by Abramson, et al.[6] was treated by a Rayleigh-type analysis with several loading modifications.[7] Agreement with experiment was obtained only when phase angles of circulation functions were arbitrarily shifted.

A modal analysis of the Abramson experiment using modified lift-slope and center-of-pressure values was conservative by about 20 percent.[8] Comparisons between the two experimental configurations were made recently by Rowe,[9] who applied various modifications of lifting surface theory to lumped parameter structural representations. None of the modifications was successful for both experiments.

It is not clear from the above studies exactly what aspects of airfoil flutter theory are at fault in describing hydrofoil flutter behavior, although the Rowe analysis suggested that the hydrodynamic rather than the structural representation was deficient. Another series of flutter

experiments has been performed in which one possible source of difficulty has been eliminated: the spanwise variation of hydrodynamic and structural parameters. Henry[10] and Cieslowski[11] have independently flutter tested two-degree-of-freedom hydrofoils in two-dimensional flow. The Henry results showed that flutter predictions using classical Theodorsen two-dimensional loading[12] were unconservative at low mass ratios approximating the hydrofoil regime but were conservative at intermediate mass ratios. Although Cieslowski reported conservative results in the low mass ratio regime, he did not use in-air torsional frequencies to calculate reduced speeds as required by theoretical assumptions, nor did he include the mass parameter β. When the correct analysis is applied, the Cieslowski results also lead to a flutter prediction that is unconservative in the low mass ratio regime and conservative at higher mass ratios. The two-degree-of-freedom hydrofoils used in these tests were well represented structurally by the equations of motion used. Therefore the unconservative flutter predictions in the hydrofoil regime, which are unacceptable for practical applications, resulted from inadequacies in the hydrodynamic loading formulation. The inadequacy may not have resided entirely in the Theodorsen loading theory since some spanwise variation in loading was undoubtedly present.

The results of Henry and Cieslowski also give an indication of the validity of the Theodorsen "representative section" flutter theory[13] in the hydrodynamic flow regime. This theory assumes that a three-dimensional wing has the same flutter characteristics as a two-dimensional foil with the profile and structural properties of the wing at approximately three-quarters of the semispan from the wing root. Representative section flutter theory has been used successfully for simple, high aspect ratio airfoils,[13,14] and gives flutter predictions that are generally conservative. The two-dimensional hydrofoils tested by Henry and Cieslowski simulated ideal representative sections. However, the predictions of Theodorsen theory were unconservative in the low mass ratio range for these hydrofoils.

It would be expected, therefore, that representative section flutter theory based on Theodorsen loading would not accurately predict the flutter characteristics of simple, high aspect ratio hydrofoils. A number of calculations demonstrated that this is indeed the case. Using the examples mentioned above, representative section theory was shown to be grossly

unconservative for the hydrofoils tested by Baird,[3] and an unpublished calculation by the author has given a prediction that is unconservative by 35 percent for the Abramson hydrofoil. Because of the failure of the two-dimensional theory, as well as the qualitative similarity between results for two- and three-dimensional hydrofoils, however, one cannot rule out the possibility that a successful two-dimensional flutter theory could serve as a basis for a successful representative section theory in the hydrodynamic flow regime. Further analysis of the simulated two-dimensional configuration would seem to be required.

In addition to the flutter characteristics of fully wetted hydrofoils, there are many aspects of cavitating hydrofoil flutter behavior that are not fully understood. Although existing hydrofoil craft are generally operated in the subcavitating regime, it is expected that future craft will be intentionally or unintentionally operated with substantial cavitation on their struts and foils. Ship control surfaces are also subject to cavitation, as was discussed in Reference 1. Cavitation produces radically different loading from fully wetted flow, and flutter predictions based on loads for cavitating flow indicate that substantial changes in flutter speed may occur with cavitation as a function of cavity length and separation point relative to the hydrofoil chord. Since the changes in flutter speed caused by cavitation may be favorable as well as unfavorable, it may be possible to exploit cavitation effects in order to achieve flutter-free high-speed design.

Also of concern to the naval architect who is designing a cavitating foil system is an unsteady loading effect produced by oscillation of cavities which are approximately 1 chord in length. Such oscillations have been reported in small-scale two-dimensional hydrofoil tests performed by Kermeen,[15] Meijer,[16] and Wade.[17] Kermeen described "severe buffeting forces" caused by "violent fluctuations" in cavity length for cavities on the order of 0.5 to 1 chord; his photographs showed that the aft portion of the cavity was shed intermittently when cavity closure occurred on the hydrofoil. Meijer observed "heavy vibrations" for cavity lengths between 0.75 and 1 chord. Wade reported an unsteady loading effect due to cavity length oscillation for cavities of 0.6 to 1.2 chords. The hydrofoils which were tested had chord lengths of 2.77 in. (Wade), 3.0 in. (Kermeen), and

5.91 in. (Meijer). The close agreement in observed instability ranges, despite changes in hydrofoil chord length, suggests that the relationship of the cavity to the hydrofoil pressure distribution is involved. This interpretation is supported by theoretical considerations presented by Guerst.[18] Since pressure distributions on full-scale control surfaces and hydrofoils are similar to model pressure distributions, there is reason to believe that cavity-induced load oscillations would occur in the full-scale regime. Excessive vibration and structural fatigue could be caused by such load oscillations.

This report presents the results of two hydrofoil tests which were done in an extension of the Cieslowski flutter experiments to cavitating flow. A semiwedge hydrofoil model was used to produce cavitation. The first test was conducted in the NSRDC high-speed towing basin[19] in July and August of 1966. Both flutter and cavity-induced oscillation were obtained. In an attempt to obtain additional flutter data, a second test was conducted in the NSRDC 24-in. variable-pressure water tunnel[19] in February and March of 1968, using the same foil and foil suspension. Only cavity-induced oscillation was obtained.

The flutter results obtained in the high-speed towing basin are compared with flutter theories which are appropriate to their cavitation regime. These comparisons should indicate the validity of the hydrodynamic loading theories which have been developed for cavitating flow in the structural and flow parameter range applicable to hydrofoil flutter. Flutter for cavities approximately 1/2 chord in length is compared with predicted values based on the work of Steinberg and Karp[20] and of Kaplan.[21] Flutter for cavities several chords in length is compared with predicted values based on the work of Woods[22] and of Kaplan and Henry.[23] Cavity-induced foil oscillations are discussed in terms of forced oscillations of a coupled two-degree-of-freedom elastic system. Several recommendations are given for further experimental and theoretical studies.

TWO-DEGREE-OF-FREEDOM HYDROFOIL SYSTEM

Both experimental tests were made using the same hydrofoil test model and two-degree-of-freedom hydrofoil suspension. Different test

sections were used in the two facilities to produce two-dimensional flow over the hydrofoil. The test sections will be described along with test procedures and results from each test.

SEMIWEDGE HYDROFOIL MODEL

A semiwedge hydrofoil made of solid titanium was used as a test model. The dimensions of the test model are given in Figure 1. The sharp leading edge was intended to produce a cavity which separated from the foil at the leading edge. For maximum strength, the foil and mounting bosses at each end were made from a single piece of material.

TWO-DEGREE-OF-FREEDOM FOIL SUSPENSION

A system of flexures was used to limit foil motion to two degrees of freedom: the heave mode, which is translation normal to the flow, and the pitch mode. The mechanism is shown schematically in Figure 2. Each end of the hydrofoil was held by an inner housing which could rotate relative to an outer housing with a torsional stiffness determined by the pitch flexures. Heave stiffness was governed by a large coil spring (two springs were used, one inside the other) in addition to the heave flexures. The heave flexures secured the housings against drag and prevented rotation of the outer housing. The suspensions were installed on the outside of parallel wall test sections, with the foil mounting bosses extending through a circular hole in each wall to the suspensions. The foil was centered in the wall openings at all run velocities by adjusting the coil spring compression to cancel the steady component of the lift. The wall openings acted as mechanical stops to heave motion, allowing the foil a $\pm$1/2-in. amplitude. Pitch motion was limited to $\pm$8 deg by pins in the housing assemblies. The foil angle of attack was controlled by a worm gear within each inner housing and could be varied over 360 deg.

The foil suspension may be characterized by the structural parameters shown in Figure 3. The hydrofoil rotates about its pitch axis, which is located a distance ab aft of midchord, where b is the semichord. For this type of suspension, a is determined by the hydrofoil model; the semiwedge hydrofoil used in the present experiment had a = -0.4, which is equivalent to a pitch axis located 30 percent of the chord aft of the leading edge.

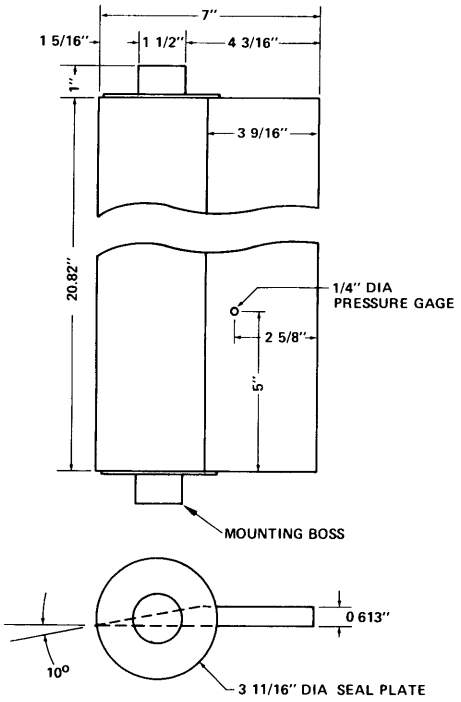

Figure 1 – Semiwedge Hydrofoil Model

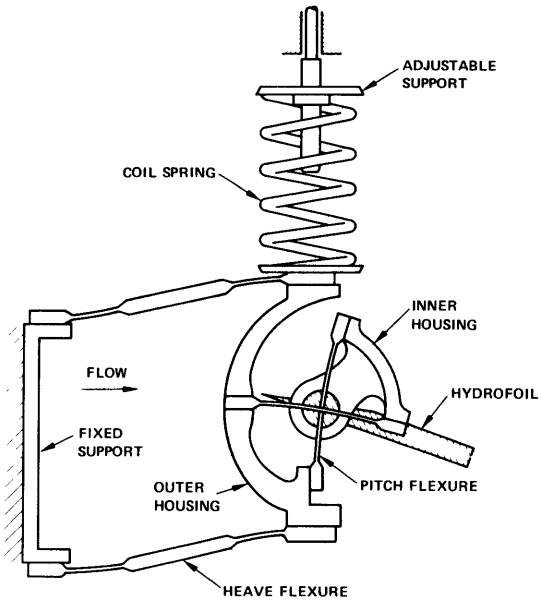

Figure 2 – Two-Degree-of-Freedom Hydrofoil Suspension

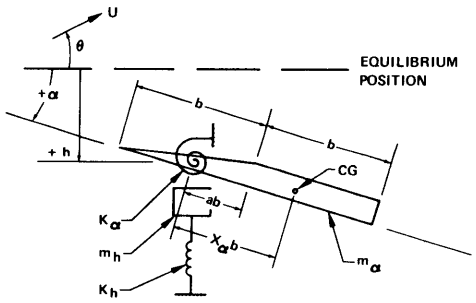

STRUCTURAL PARAMETERS	MASS RATIOS		
	1 44	2.29	3 31
f_h (Hz)	15.22	12.08	10 06
f_α (Hz)	21.82	17 68	15 15
r_α	1 320	1 048	0 958
β	0 449	0.638	0.771

NOTE VALUES FOR OTHER STRUCTURAL PARAMETERS WERE AS FOLLOWS· a = -0 4 b = 0 292 FT, K_α = 1640 9 FT-LB/RAD, K_h = 11,976 LB/FT, AND › = 1.735 FT

Figure 3 – Semiwedge Hydrofoil Model Parameters

The center of gravity of all rotating components is located x_α semichords aft of the pitch axis; x_α, called the mass unbalance, is continuously and independently varied by rotating four eccentric weights about two shafts (not shown in Figure 2) attached to the inner housings. The four eccentric weights, two concentric weights, the inner housings, and the foil itself determine the rotating mass m_α and the radius of gyration r_α. The nonrotating mass m_h consists of the outer housing mass plus one-third the mass of the coil springs, with β being the ratio $m_\alpha/(m_h + m_\alpha)$. Mass ratio μ is defined as the ratio of the total mass to the mass of a cylinder of water circumscribing the foil, $(m_h + m_\alpha)/\pi\rho b^2 s$. The rotational spring constant K_α is determined by the pitch flexures, and the translational spring constant K_h is determined by the coil springs and the heave flexures.

Spring constants K_h and K_α were obtained by static applications of forces and moments to the hydrofoil. The first moments of inertia S_α (expressed as mass unbalances x_α) were determined by combining the first moments of the individual eccentric weights and the hydrofoils. The second moments of inertia I_α (expressed as radii of gyration r_α) were calculated from the measured in-air natural frequencies and were compensated for the experimentally determined added mass and moment of the suspensions but not of the foil. The structural parameter values given in Figure 3 therefore approximate the in-vacuum characteristics of the hydrofoil system needed for theoretical analysis.

The above-described foil suspension design placed certain limitations on the variation of structural parameters. Only x_α and α could be changed independently of all other parameters. Changes in μ, accomplished by changing the eccentric weights, produced changes in r_α, β, f_h, and f_α. Since several parameters were thus linked to mass ratio, it has been found convenient to specify structural configurations in terms of mass ratio μ, mass unbalance x_α, and angle of attack α. A complete list of the other parameter values is given in the tabulation of Figure 3.

EQUATIONS OF MOTION

The equations of motion for the coupled, two-degree-of-freedom hydrofoil system in two-dimensional flow are as follows:

$$(m_h + m_\alpha)\ddot{h} + S_\alpha \ddot{\alpha} + K_h h = -L$$
$$I_\alpha \ddot{\alpha} + \beta_\alpha \ddot{h} + K_\alpha \alpha = M \qquad [1]$$

where dots indicate differentiation with respect to time. The hydrodynamic lift L and moment M are functions of the pitch and heave coordinates and the flow parameters. Flutter characteristics are obtained by determining the flow parameters which satisfy Equations [1] for simple harmonic motion, which corresponds to zero damping.

INSTRUMENTATION

Foil motion was monitored by pen recordings of the output of strain gages attached to the pitch and heave flexures. Several runs in the 24-in. water tunnel were also recorded on magnetic tape.

A pressure gage designed to withstand the effects of cavitation was mounted on the top surface of the foil, as shown in Figure 1, and its output monitored by pen recordings. The gage survived all testing in the high-speed basin but failed after several hours of exposure to cavity conditions in the 24-in. water tunnel.

CAVITATING FLUTTER TEST IN TOWING BASIN

The hydrofoil model and suspension described above were first tested in the high-speed towing basin using a two-dimensional test section which was drawn by a towing carriage. The foil suspension and test section had been previously used to study flutter of a noncavitating hydrofoil.[11]

TWO-DIMENSIONAL TEST SECTION

Large parallel surface-piercing end plates 21 in. apart were used to produce two-dimensional flow past the semiwedge hydrofoil. The end plates were 58 in. long and had sharp leading edges. The leading edge of the hydrofoil was located 37 in. aft of the end plate leading edges. At the foil test depth of 1 chord (7 in.), the bottom of the end plates was 25.5 in. below the water surface. Faired boxes on the outside of the end plates

contained the foil suspension systems. In order to minimize flow blockage, each suspension box was located entirely within the Kelvin wave envelope emanating from the leading edge of the end plates.

The end plates were attached to a superstructure which was bolted to the high-speed towing carriage (NSRDC Carriage 5). In addition to the superstructure bracing, it was found necessary to connect the bottom part of the end plates with three faired braces to maintain the distance of separation against forces caused by the effective camber of the end plate-box combination. Towing speeds were held to a maximum of approximately 30 knots in view of the large drag force which was present.

EXPERIMENTAL PROCEDURE

Since flutter characteristics were desired for a foil under cavitating conditions, the foil was operated at relatively high angles of attack, from 7 to 10 deg, to produce cavities which separated from the sharp leading edge of the foil. A high pressure air system, which injected air at 100 psi into the flow through a 3/8-in. opening just forward of the leading edge of the foil, was used to produce long cavities which were vented to the atmosphere. Direct observation of cavity characteristics was not possible, but still photographs or high-speed motion pictures were taken of many runs.

Flutter speed boundaries were determined by towing the foil at several speeds on successive runs until flutter occurred. Additional runs were made to define the critical flutter speeds more precisely. Carriage speeds were determined by reference to digital printouts generated by the carriage control system at the rate of two per second.

CAVITATION CHARACTERISTICS

Several discontinuities in the steady-state loading of the foil were observed during testing. These discontinuities took the form of a rapid change in the steady heave and pitch amplitudes as well as in the pressure gage reading. The steplike change did not appear to be related to unsteady motions that may have been taking place at the time. Subsequent analysis indicated the occurrence of four distinct cavity configurations among which abrupt transitions occurred. Each cavity configuration exhibited a

characteristic cavity length and cavitation number. Flutter characteristics of the foil system were found to depend on which cavity configuration was present. Varying amounts of cavity ventilation to the free surface, through and around the end plates, appeared to be responsible for the types of cavities that were formed. Therefore, the cavitation characteristics of the foil-end plate vehicle will be discussed before the flutter results are reported.

Pressure data exhibiting three of the four cavitation regimes are shown in Figure 4 (the fourth type of cavitation did not give meaningful pressure readings). High-speed motion pictures permitted viewing the flow phenomena at 1/16 of actual speed and gave a clear indication of the cavity conditions which accompanied each of the three branches of data in Figure 4. The fourth type of cavity was observed in still photographs. The cavitation regimes are listed in Table 1 in order of increasing cavity length.

Cavitation Regime 1 (1/2 Chord in Length)

The first type of cavitation to be discussed had a cavity length of less than 1/2 chord; see Figure 5. As might be expected, these relatively short cavities occurred during relatively low-speed runs, from 19.2 to 22.9 knots. These were probably vapor cavities without ventilation. Cavitation number based on water vapor pressure σ_v ranged from 2.03 to 1.43. The shape of the cavity, which showed little spanwise variation, may have been influenced by the ridge on the top surface of the semiwedge foil. Large-amplitude, nonperiodic pressure oscillations were recorded by the pressure gage downstream in the wake of the cavity. No pressure data for this regime appear in Figure 4. No reentrant jet was visible.

Cavitation Regime 2 (1 Chord in Length)

The second type of cavitation corresponded to a cavity extending to the trailing edge at the midspan of the foil but shrinking to zero length at the end of the foil (Figure 6). A strong reentrant jet was present at the midspan of the foil. Cavitation along the base of the foil was also

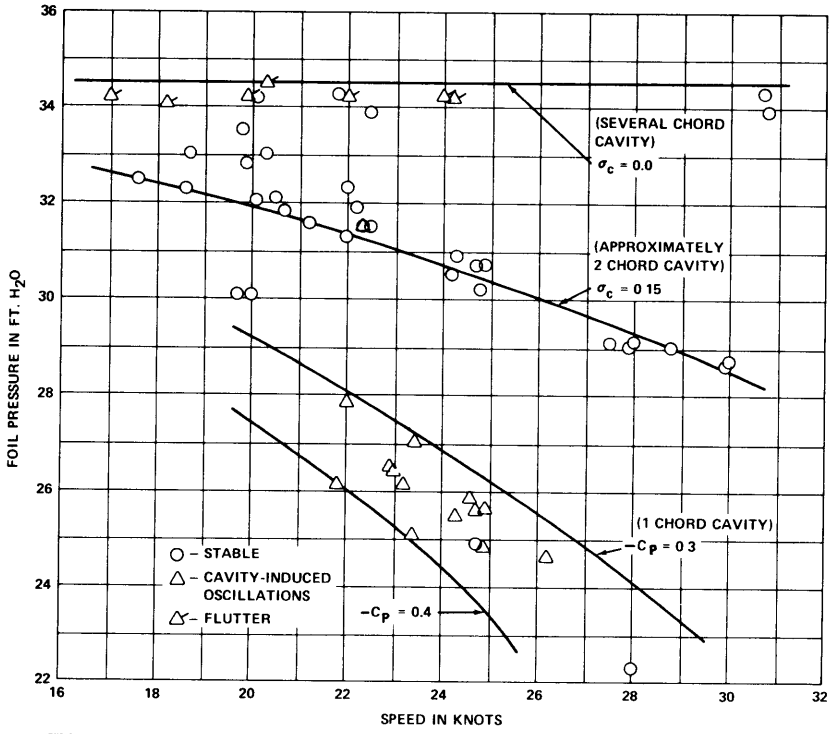

Figure 4 – Pressure at Foil Pressure Gage as a Function of Towing Carriage Speed

TABLE 1

Cavitation Regimes Observed in High-Speed Towing Basin Test

Cavitation Regime	Cavity Length chords	Cavitation Number	Amount of Ventilation	Comments
1	Less than 0.5	σ_V = 1.43 to 2.03	Probably none	See Figure 5
2	1.0	σ_V = 0.96 to 1.58	Unknown	See Figure 6
3	~2.0	σ_C = 0.15	Partial	See Figure 7
4	Several	σ_C = 0.007 to 0.047	Full	See Figure 8

evident. Foil pressure data fell between negative pressure coefficients of 0.3 and 0.4, as shown in Figure 4. This type of cavitation occurred for σ_v values of 1.58 to 0.96.

The pressures measured in this cavitation regime, approximately 26 ft of water, could be interpreted in two ways: either (1) a partially ventilated cavity was covering the pressure gage or (2) the gage was in fully wetted flow on the suction side of the hydrofoil. Manometer measurements showed that the faired boxes on the outside of the end plates drained completely in the course of a run, so that air was entering the flow at the ends of the foil through the openings in the end plates. The air is visible along the ends of the foil in Figure 6. It is not certain whether or not air is entering the cavity. Examination of still photographs and motion pictures of the flow situation indicated that the cavity did not cover the pressure gage. The data analysis assumed that pressure coefficients near 0.35 indicated Cavitation Regime 2.

Cavitation Regime 3 (2 Chords in Length)

The third cavitation regime was characterized by a cavity about 2 chords in length with little distinguishable spanwise variation; see Figure 7. Pressure data yielded a negative pressure coefficient of 0.15, based on measured pressures of 28.6 ft of water and above. Since the cavity covered the pressure gage, the negative pressure coefficient for this cavity configuration was σ_c, the cavitation number based on cavity pressure. The high pressure readings indicated partial ventilation of the cavity. Ventilation apparently occurred through the openings in the end plates and was restricted by the foil mounting boss, the seal plate, and the water flow at each wall. This type of cavity was formed by a sudden joining of the partial cavity of Cavitation Regime 2 with the airstream entrained in the flow along the wall. Subsequent enlargment of the cavity was evident in the motion pictures; it was characterized by a jump in foil amplitudes and a rise in pressure as well. This type of cavity was increasingly likely to be formed as towing speeds increased.

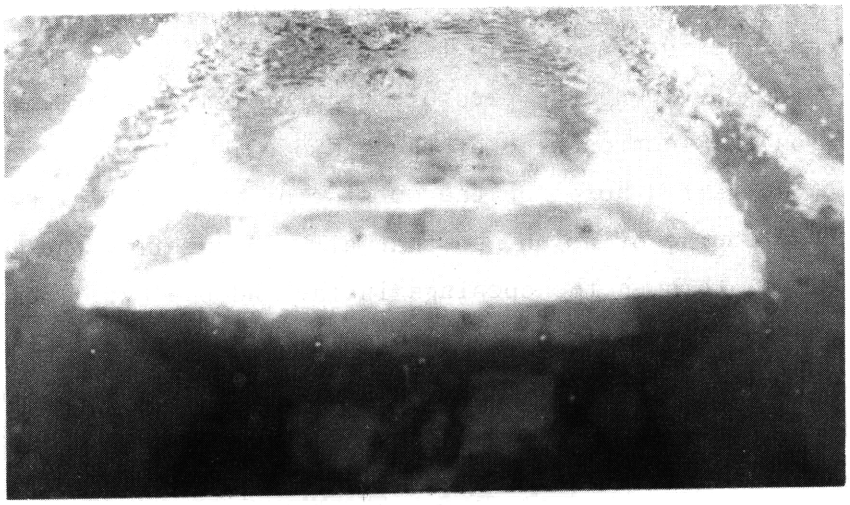

Figure 5 – Hydrofoil in Cavitation Regime 1
$\sigma_v = 1.92$

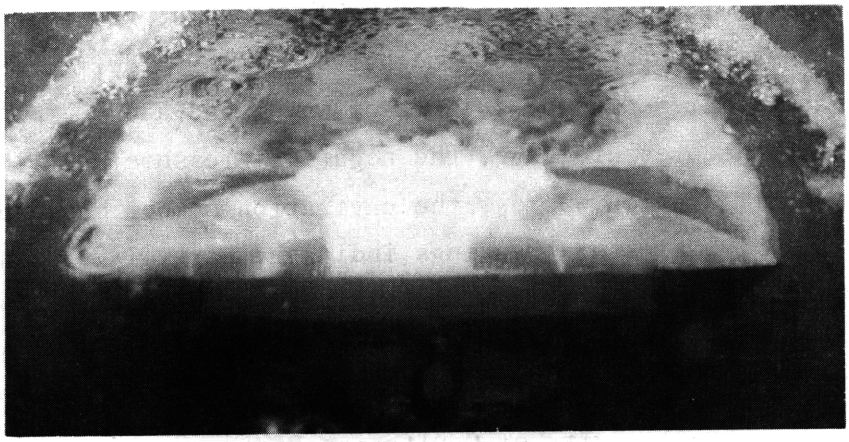

Figure 6 – Hydrofoil in Cavitation Regime 2
$\sigma_v = 1.42$

Cavitation Regime 4 (Several Chords in Length)

By injecting high-pressure air just forward of the foil, it was possible to form the fourth type of cavity encountered. A long cavity appeared which was vented to the atmosphere; see Figure 8. The spanwise waves which are visible in the top surface of the cavity in Figure 8 had a frequency of approximately 200 Hz and are thought to have been caused by spanwise bending of the foil, which was calculated to have a frequency of the same order of magnitude. The formation of the vented cavity was accompanied by a large decrease in the vertical position of the foil (reflecting a decrease in steady lift) and a rise in cavity pressure to just below atmospheric; σ_c values ranged from 0.047 to 0.007. The cavity now extended to the rear of the end plates. The injected air may have linked the foil cavity with surface-vented cavities formed at the rear of the end plates, permitting air to flow forward and enter the foil cavity.

Ventilation was obtained by air injection at speeds as low as 14.3 knots, but, in general, the speed at which ventilation occurred was related to the maximum towing carriage speed on a given run: higher run speeds produced higher ventilation inception speeds. Carriage acceleration, which was constant until nearly full speed was reached, did not appear to be responsible for changes in ventilation inception speed. Time elapsed from the beginning of the run may have determined when ventilation would occur since draining of the faired boxes and subsequent ventilation of cavities at the rear of the end plates would have required a certain amount of time. An elapsed time effect would have produced an apparent speed dependence in view of the carriage deceleration in approaching the final smooth run speed. During carriage deceleration, the ventilated cavity persisted to speeds as low as 11 knots before collapsing. Air injection was required to maintain the surface-vented cavity configuration at speeds below approximately 18 knots. In two instances, surface ventilation occurred spontaneously without the injection of air.

The four observed cavitation patterns may be summarized in the following terms. At relatively low speeds, short vapor cavities approximately 1/2 chord in length at foil midspan were formed (σ_v = 2.03 to 1.43). At moderate speeds, cavities 1 chord in length appeared (σ_v = 1.58 to 0.96)

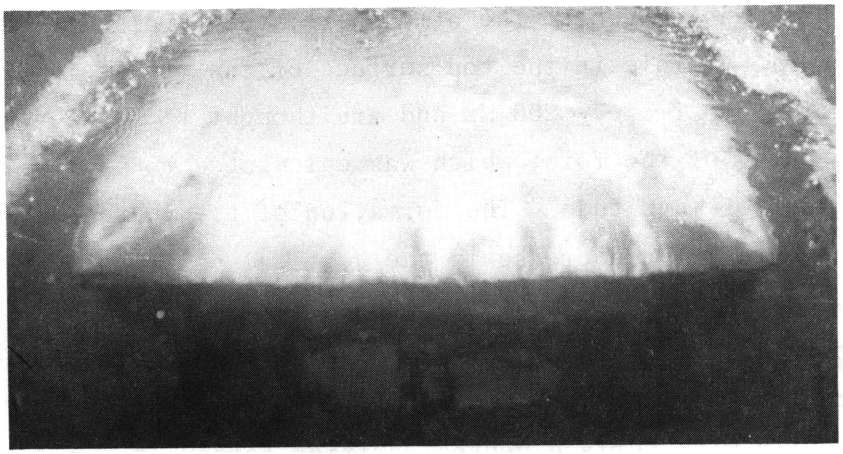

Figure 7 – Hydrofoil in Cavitation Regime 3
$\sigma_c = 0.14$

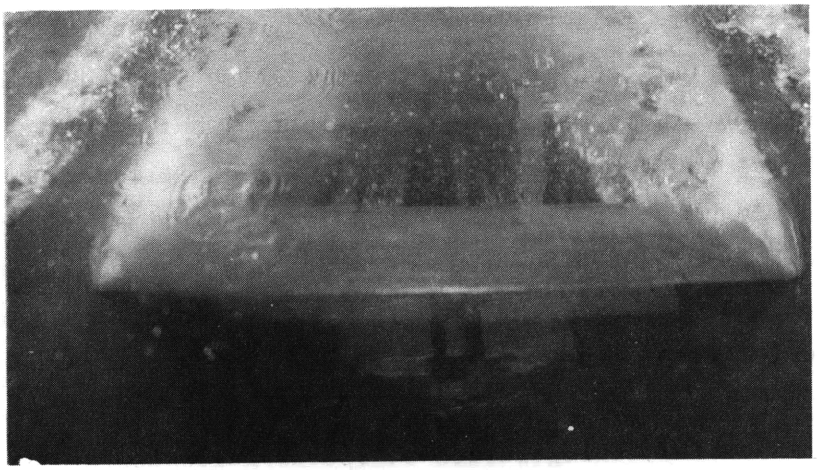

Figure 8 – Hydrofoil in Cavitation Regime 4
$\sigma_c = 0.024$

and usually became enlarged to about 2 chords due to partial venting (σ_c = 0.15). Fully vented cavities several chords in length ($\sigma_c \sim 0$) occurred if triggered at speeds ranging from 14 to 30 knots.

It should be noted that the discontinuous cavity configurations described above place severe limitations on the use of the high-speed basin test section to survey the effects of cavitation. One is restricted to only four cavity lengths, which may or may not be in the region of interest. Furthermore, only the fully ventilated cavity regime can be produced at will by means of air injection; the other three types of cavities appear and disappear spontaneously. It is clear that only the fully ventilated cavity configuration can be efficiently tested in the towing basin with the present apparatus. Modification of the end plate openings to reduce or eliminate air flow would be required for testing cavities less than several chords in length.

FLUTTER RESULTS

The hydrofoil system was susceptible to flutter when in Cavitation Regime 1 (cavities shorter than 1/2 chord) and in Cavitation Regime 4 (cavities several chords in length). Flutter was evidenced by well-defined foil oscillations which occurred at and above the critical flutter speed, exhibiting the same frequency in both pitch and heave modes. The amplitudes of the oscillations grew rapidly to maximum values which remained less than those permitted by the mechanical stops, suggesting the presence of nonlinearities in the structural system and/or the flow. Table 2 gives the critical flutter boundary speeds and frequencies as well as the maximum speeds attained when flutter did not occur. Reduced flutter speeds and flutter frequency ratios are plotted in Figures 9 through 12 as a function of mass unbalance x_α for μ = 1.44, 2.29, and 3.31; flutter-free regions are indicated by vertical lines. Existing theoretical predictions are also plotted, and will be discussed below.

Flutter speeds were affected by several sources of experimental uncertainty. Because the number of test runs was limited, speed increments were not as small as desired in some cases. Carriage speed curves could not be precisely matched with oscillograph records. Acceleration effects were introduced by towing carriage acceleration before and after the run

TABLE 2

Flutter Boundaries Observed in High-Speed Towing Basin Test

Cavitation Regime	Mass Ratio μ	Mass Unbalance x_α	Angle of Attack at Rest deg	Flutter Speed U_f knots	Flutter Frequency f_f Hz	Flutter Free Speed knots
1 1/2 Chord Cavity (Figure 5)	2.29	0.563	8	21.6	17.6	---
	3.31	0.006	10	---	---	20.2
		0.315	8	22.0	14.0	---
		0.438	8	19.8	14.0	---
	3.31	0.569	10	19.24	14.7	---
4 Several Chord Cavity (Figure 8)	1.44	0.636	8	---	---	30.7
	1.44	0.700	8	---	---	31.9
	2.29	0.563	8	14.3*	20.9*	---
	3.31	0.006	10	---	---	30.8
		0.315	8	---	---	30.0
		0.438	8	20.2	16.6	---
		0.438	8	---	---	22.6**
		0.438	8	---	---	29.4**
	3.31	0.569	8	17.0	17.9	---

*Flutter boundary not established (see text).

**Flutter-free region above established flutter boundary at 20.2 knots.

Figure 9 – Reduced Flutter Speed in Partially Cavitating Flow as a Function of Mass Unbalance

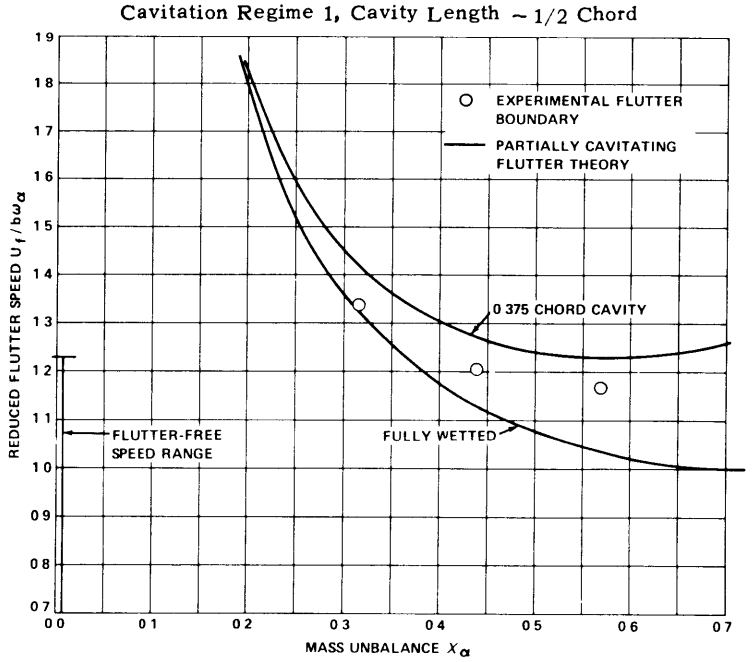

Figure 9a – $\mu = 3.31$

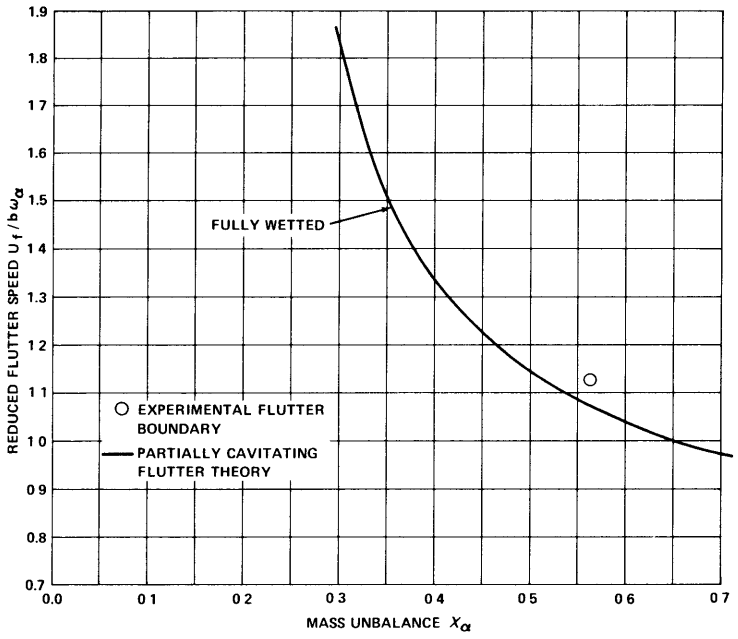

Figure 9b – $\mu = 2.29$

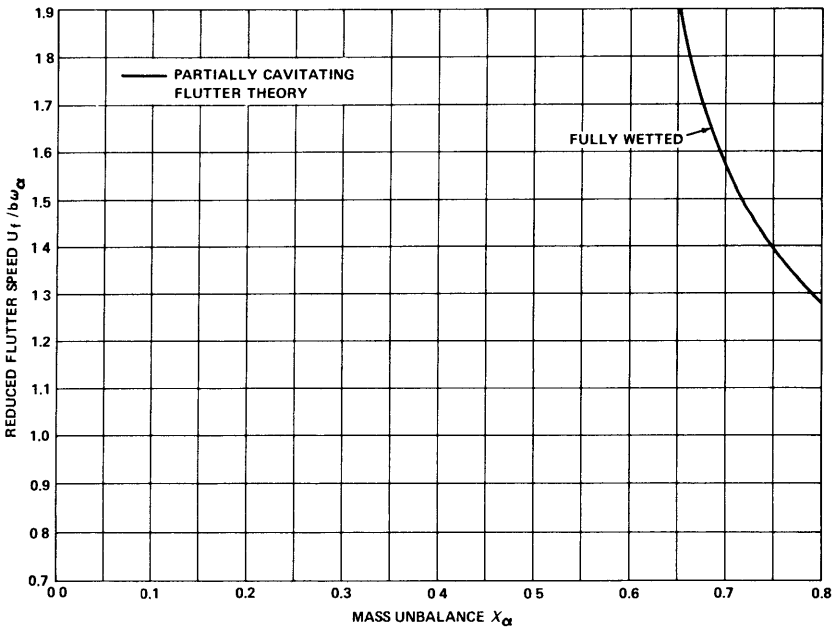

Figure 9c – $\mu = 1.44$

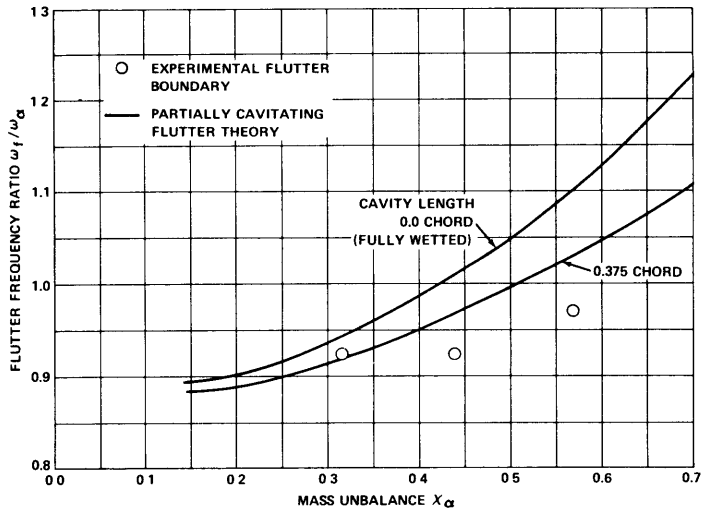

Figure 10a – $\mu = 3.31$

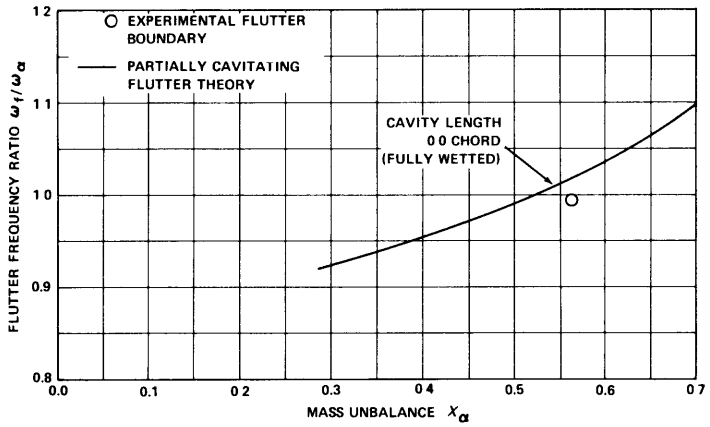

Figure 10b – $\mu = 2.29$

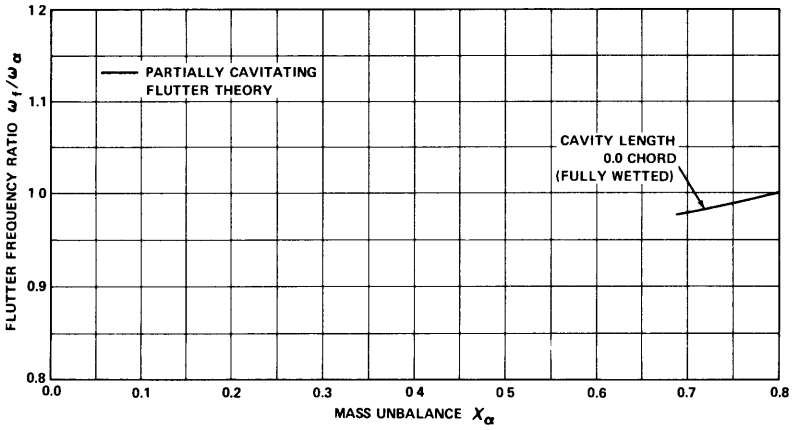

Figure 10c – $\mu = 1.44$

Figure 10 – Flutter Frequency Ratio in Partially Cavitating Flow as a Function of Mass Unbalance

Cavitation Regime 1, Cavity Length ~1/2 Chord

as well as by an overshoot in the carriage speed curve of as much as 5 percent above the nonaccelerating run speed. Positive acceleration may have acted to inhibit flutter inception since the foil accelerated through the mass ratio 3.31 flutter boundary at $x_\alpha = 0.438$ without fluttering. On the other hand, flutter persisted for several knots below inception speed during deceleration. It is estimated that the above sources of experimental uncertainty amount to ±5 percent of the flutter speed.

In addition to the above sources of experimental uncertainty, the flutter point for $\mu = 2.29$ in Cavitation Regime 4 must be considered uncertain from another standpoint. In order to determine the boundary of a flutter region accurately, a flutter-free run must be made outside the region as well as a flutter run inside the region. Since no flutter-free run was made for $\mu = 2.29$, it cannot be said that the flutter boundary was established. The value of 14.3 knots used for this boundary was the lowest actual ventilation and flutter inception speed taken from the accelerating part of the run rather than the nonaccelerating run speed as used for the other boundaries.

In both Cavitation Regimes 1 and 4, critical flutter speeds decreased and flutter frequencies increased with increasing x_α. A flutter-free region was found above the flutter boundary for $\mu = 3.31$ at $x_\alpha = 0.438$ in Cavitating Regime 4, which is shown in Figure 11a. This flutter-free region must be considered to be poorly defined since it is based on only two test runs and may have been affected, or perhaps caused by acceleration. Additional data would be needed to confirm the existence of such a region.

When the flutter results for Cavitation Regimes 1 and 4 are compared, it may be seen that for $\mu = 3.31$, the flutter speeds changed more rapidly with x_α in Regime 4. For $\mu = 2.29$, the flutter speed was substantially lower in Regime 4 than in Regime 1. Flutter frequency ratios were approximately 20 percent higher in Regime 4. No flutter was obtained for $\mu = 1.44$.

Sample records of foil motion and pressure gage output in the vicinity of flutter are given in Figures 13 through 15. Figure 13 shows the flutter motion in Cavitation Regime 1 as well as the violent pressure oscillations which were apparently caused by the cavity wake. Figure 14 illustrates the subcritical motion in Cavitation Regime 4 where the sudden disturbance

Figure 11 – Reduced Flutter Speed in Fully Ventilated Flow as a Function of Mass Unbalance

Cavitation Regime 4, Cavity Length = Several Chords

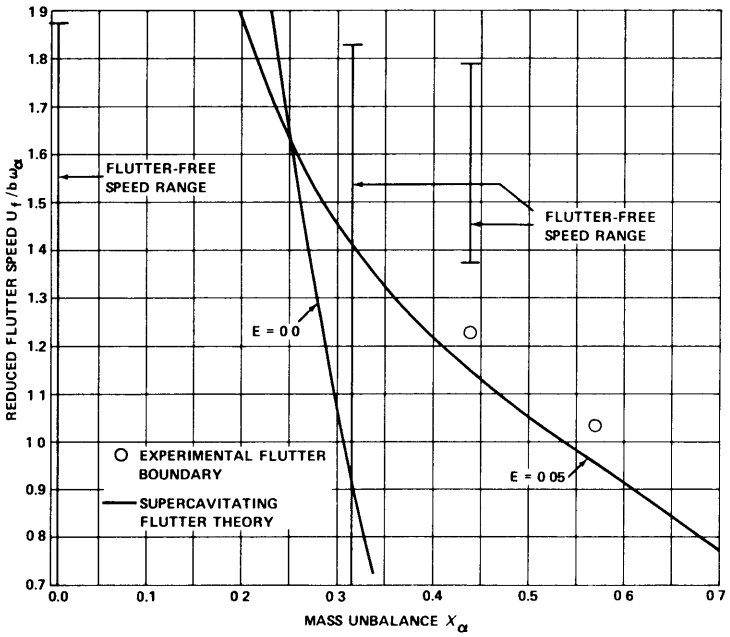

Figure 11a – $\mu = 3.31$

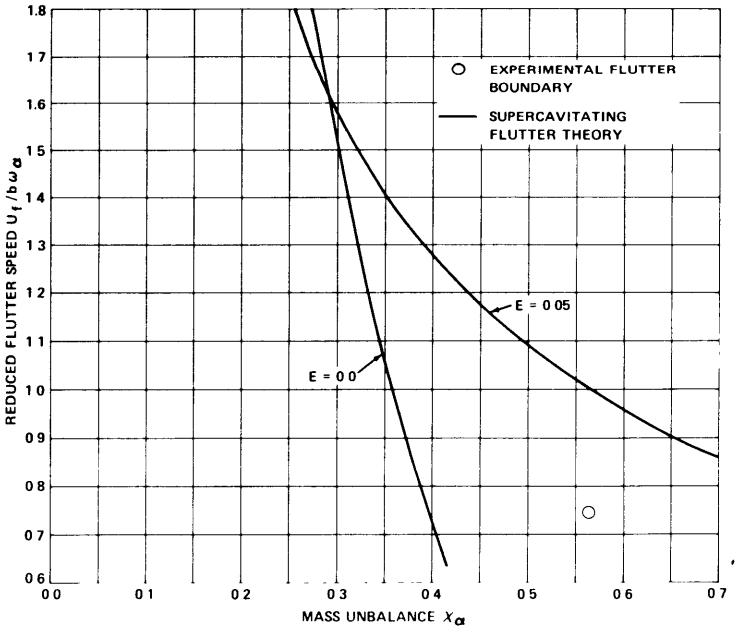

Figure 11b – $\mu = 2.29$

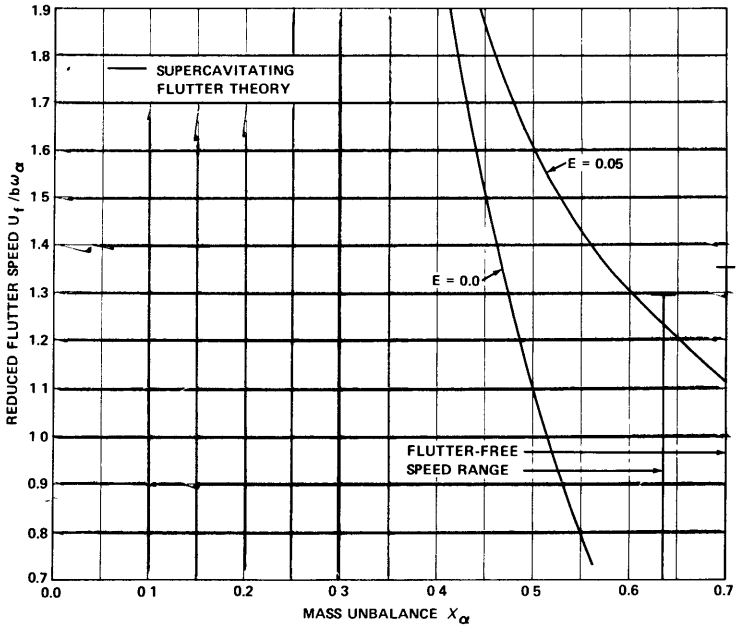

Figure 11c – $\mu = 1.44$

Figure 12 – Flutter Frequency Ratio in Fully Ventilated Flow as a Function of Mass Unbalance

Cavitation Regime 4, Cavity Length = Several Chords

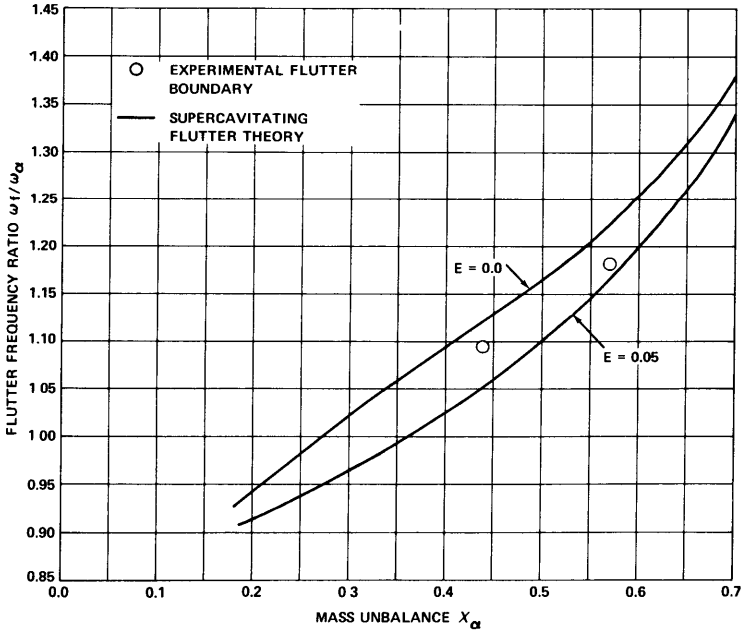

Figure 12a – $\mu = 3.31$

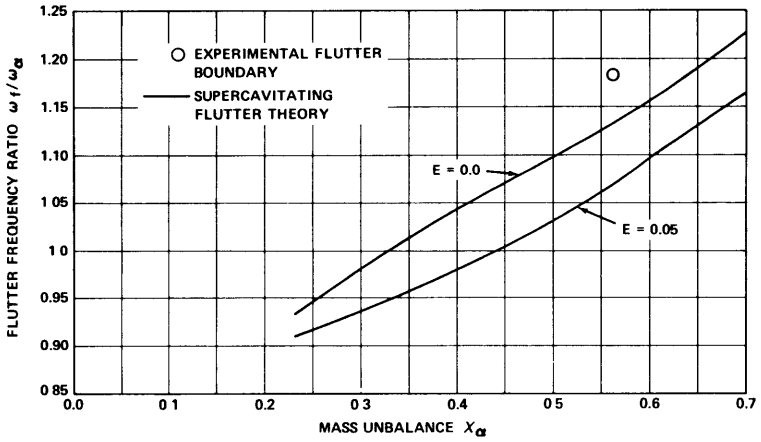

Figure 12b – $\mu = 2.29$

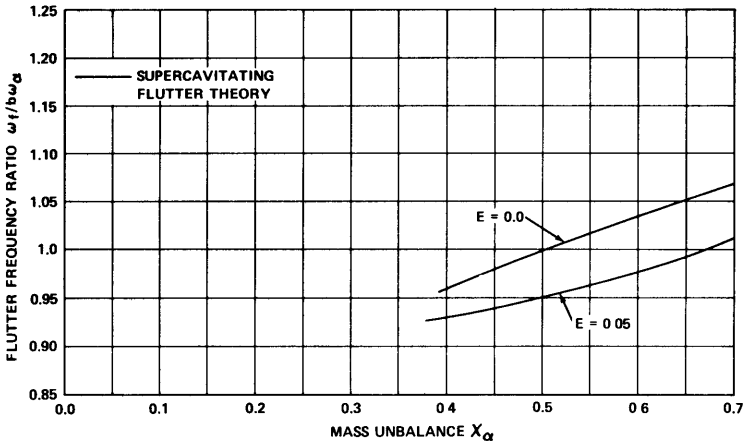

Figure 12c – $\mu = 1.44$

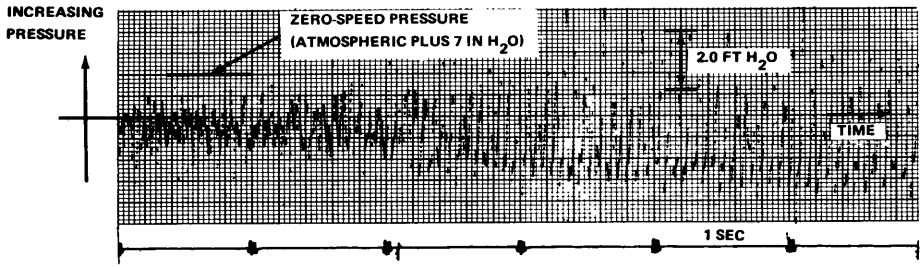

Figure 13a – Pressure on Hydrofoil

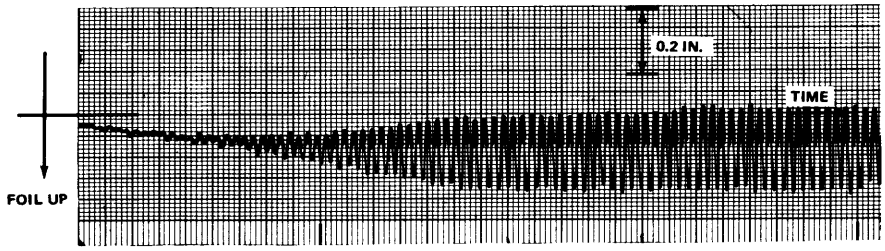

Figure 13b – Heave Amplitude

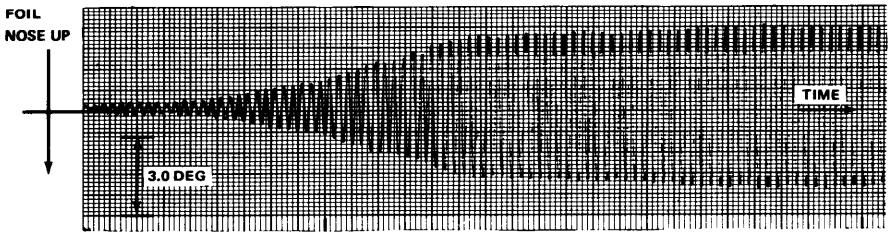

Figure 13c – Pitch Amplitude

Figure 13 – Oscillograph Records of Pressure, Heave, and Pitch Amplitudes at a Velocity above the Flutter Boundary in Partially Cavitating Flow

Cavitation Regime 1

$\mu = 3.31$, $x_\alpha = 0.569$, $U/b\omega_\alpha = 1.24$, cavity length ~ 1/2 chord.

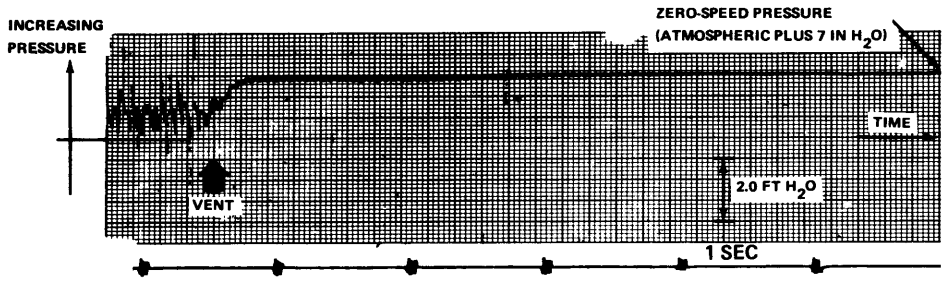

Figure 14a – Pressure on Hydrofoil

Figure 14b – Heave Amplitude

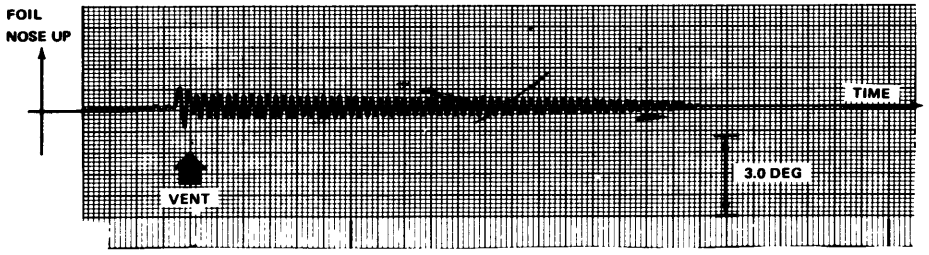

Figure 14c – Pitch Amplitude

Figure 14 – Oscillograph Records of Pressure, Heave, and Pitch Amplitudes at a Velocity below the Flutter Boundary during Transition from Cavity Length of One to Several Chords

Cavitation Regimes 2 to 4

$\mu = 3.31$, $x_\alpha = 0.438$, $U/b\omega_\alpha = 1.16$

caused by ventilation was damped out. Figure 15 shows the increase in oscillation amplitude which occurred at a slightly higher speed above the flutter boundary.

The relative phase angle between the pitch and heave modes during flutter could not be determined because foil motions were recorded at too slow a recording chart speed. No attempt was made to determine amplitude ratios.

CAVITY-INDUCED OSCILLATION

Foil motion in Cavitation Regime 2 was characterized by pitch oscillation of large but varying amplitude accompanied by heave oscillation of very small amplitude, as illustrated in Figure 16. The oscillation frequency ranged from 15.95 Hz at 21.8 knots to 16.6 Hz at 24.9 knots. This oscillation occurred for the structural parameters $\mu = 3.31$, $x_\alpha = 0.006$, and $\alpha = 10$ deg at zero speed. All runs displaying this type of oscillation are plotted in Figure 4. This oscillation did not exhibit a critical speed boundary below which no oscillation was present, but rather the oscillations occurred almost invariably when the 1-chord cavity of Regime 2 occurred. Of course, such a boundary may have existed below the minimum speed for which Regime 2 cavitation was obtained. However, the results obtained in the 24-in. water tunnel test (discussed later) suggest that this oscillation was induced by cavity length oscillations which are typical of cavities approximately 1 chord in length. If this is a valid interpretation, the variations in pitch amplitude may have indicated the presence of more than one frequency. Theoretical considerations support this interpretation since flutter would be extremely unlikely at $x_\alpha = 0.006$.

STABLE CONDITION

Regime 3 cavitation, characterized by a cavity approximately 2 chords in length, occurred only for the structural parameter values $\mu = 3.31$, $x_\alpha = 0.006$, and $\alpha = 10$ deg. Foil motion was stable at all speeds to 30 knots in this cavitation regime. As mentioned above, however, flutter is not likely to occur at $x_\alpha = 0.006$. A typical record of foil motion in this regime is shown in Figure 17. Upon transition from Regime 2 to Regime 3, there was a drop in heave amplitude and an increase in pressure

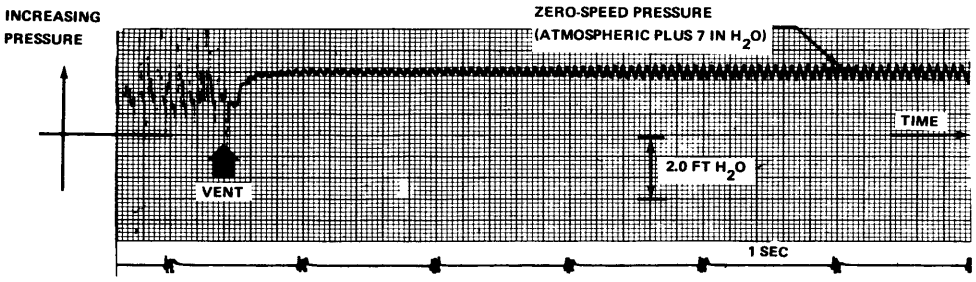

Figure 15a – Pressure on Hydrofoil

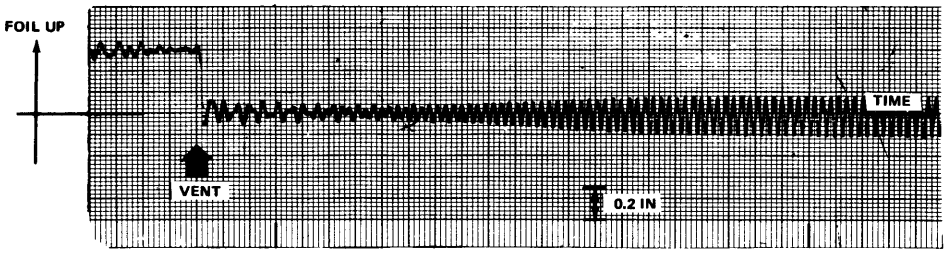

Figure 15b – Heave Amplitude

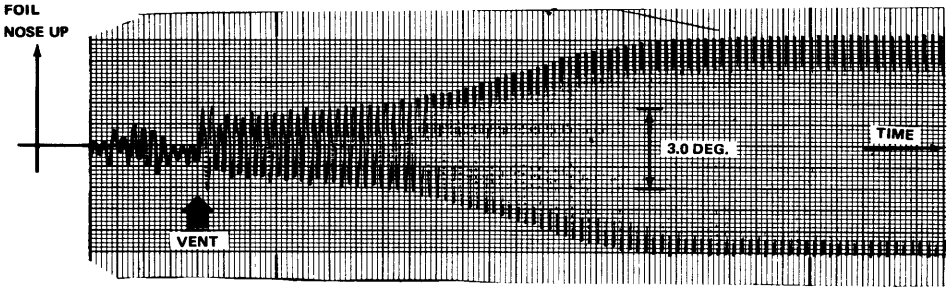

Figure 15c – Pitch Amplitude

Figure 15 – Oscillograph Records of Pressure, Heave, and Pitch Amplitudes at a Velocity above the Flutter Boundary during Transition from Cavity Length of One to Several Chords

Cavitation Regimes 2 to 4

$\mu = 3.31$, $x_\alpha = 0.438$, $U/b\omega_\alpha = 1.17$

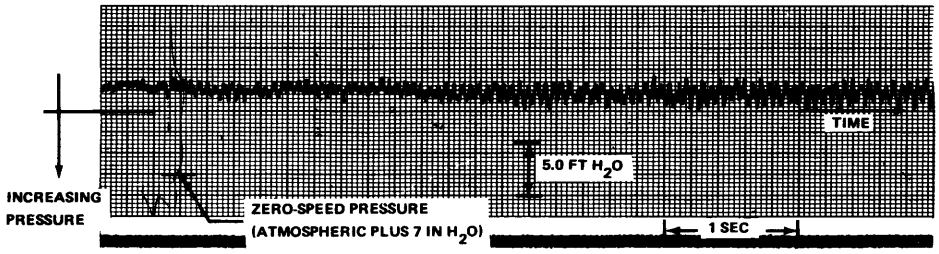

Figure 16a – Pressure on Hydrofoil

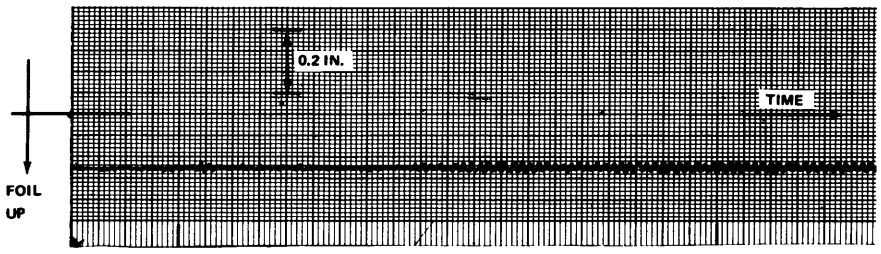

Figure 16b – Heave Amplitude

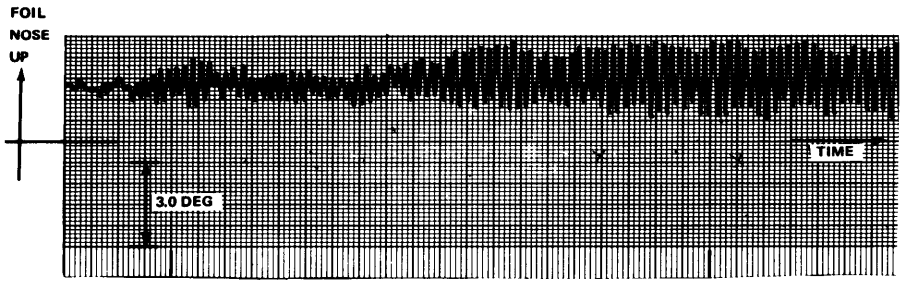

Figure 16c – Pitch Amplitude

Figure 16 – Oscillograph Records of Pressure, Heave, and Pitch Amplitudes during Cavity-Induced Foil Oscillations for a 1-Chord Cavity

Cavitation Regime 2

$\mu = 3.31$, $x_\alpha = 0.006$, $U/b\omega_\alpha = 1.35$

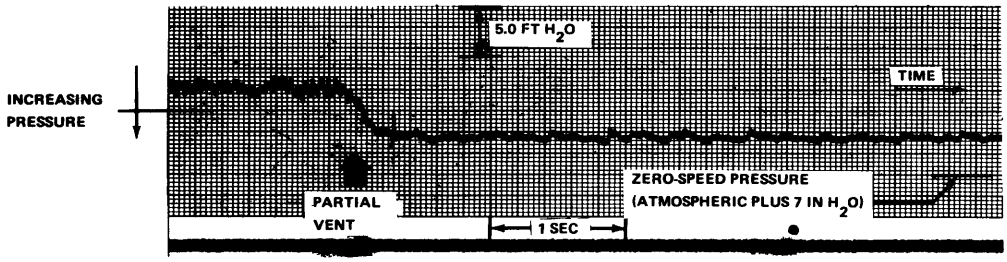

Figure 17a – Pressure on Hydrofoil

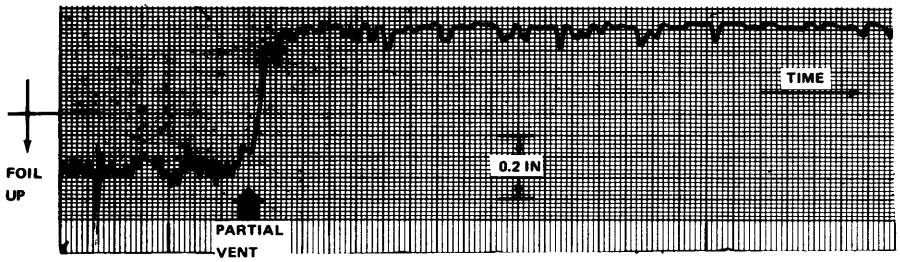

Figure 17b – Heave Amplitude

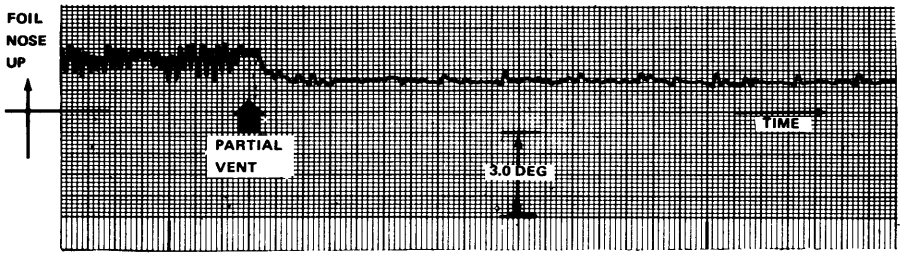

Figure 17c – Pitch Amplitude

Figure 17 – Oscillograph Records of Pressure, Heave, and Pitch Amplitudes in the Stable Condition Following Transition from 1- to 2-Chord Cavity Length

Cavitation Regimes 2 to 3

$\mu = 3.31$, $x_a = 0.006$, $U/b\omega_a = 1.45$

due to partial ventilation as the cavity changed from 1 to 2 chords in length. The foil motion appeared to be highly damped since the impulse caused by partial ventilation produced no sustained oscillations. The foil was not contacting the bottom heave stop in this configuration.

THEORETICAL FLUTTER ANALYSIS

Theoretical flutter boundaries for both partially cavitating and supercavitating flow have been calculated using Equation [1], with appropriate hydrodynamic load expressions obtained from the literature. For partially cavitating flow, load coefficients given by Steinberg and Karp[20] were combined with the flutter determinant used by Kaplan.[21] The load coefficients were supplemented by a four-point interpolation which proved to be unreliable because insufficient coefficients were available. For supercavitating flow, load expressions given by Woods[22] were used in the flutter formulation published by Kaplan and Henry.[23] Loading was calculated by a computer program of the Wood theory written by Patton and Borden,[24] which yielded exact results. Both load theories include the classical Theodorsen loading[12] as a special case.

Partially Cavitating Hydrofoil Flutter

Steinberg and Karp[20] have derived the unsteady loading on a hydrofoil in the presence of a cavity extending up to 0.75 chord aft of the leading edge. The load expressions were evaluated[20] for only a limited number of reduced frequencies and for 0.125-chord cavity-length increments. The calculation of flutter boundaries for the present analysis necessitated determining load coefficients for additional values of reduced frequency. The use of a four-point interpolation based on the known coefficients produced inconsistent results in the reduced frequency range of 0.5 to 1.0. Since it was not feasible to make an exact computation of the necessary load coefficients at this time, flutter calculations for mass ratio 1.44 and 2.29 will not be presented. It is felt, however, that mass ratio 3.31 calculations may be sufficiently reliable to indicate general trends. Therefore flutter speed boundaries for $\mu = 3.31$ are shown in Figure 18 as a function of cavity length for three values of x_α used experimentally.

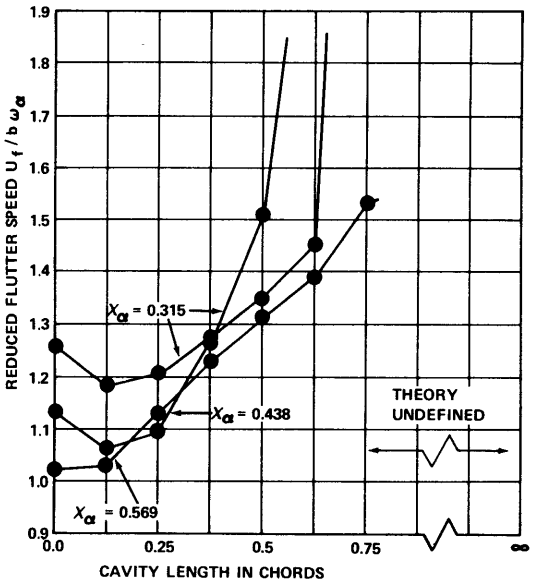

Figure 18 – Theoretical Reduced Flutter Speed as a Function of Cavity Length and Mass Unbalance in Partially Cavitating Flow

$\mu = 3.31$, $x_\alpha = 0.315, 0.438, 0.569$.

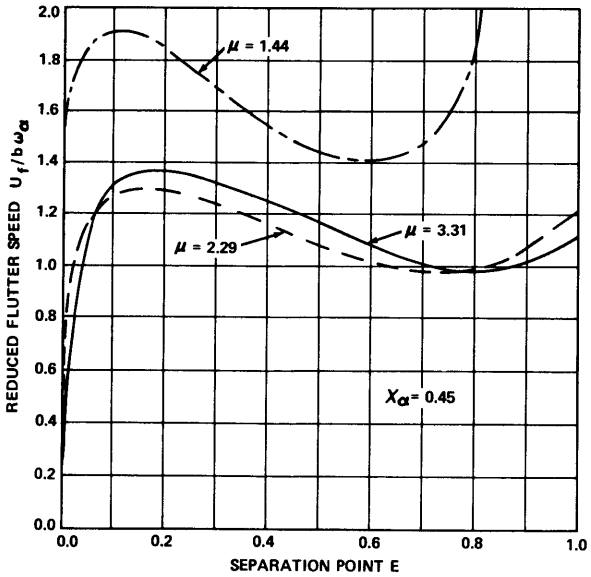

Figure 19 – Theoretical Reduced Flutter Speed as a Function of Cavity Separation Point and Mass Ratio

$\mu = 1.44, 2.29, 3.31$; $x_\alpha = 0.45$.

Within the accuracy of the calculation, the partially cavitating flutter boundaries begin at Theodorsen values for zero cavity length. As the cavity length increases from zero, a slight decrease in flutter speed is predicted, after which the critical flutter speed increases rapidly, apparently becoming infinite at 0.75 chord cavity length.

Theoretical flutter speed boundaries and frequency ratios are plotted as functions of x_α in Figures 9 and 10 along with the experimental flutter points. The exact Theodorsen theory was used for zero cavity length curves whereas the 0.375 chord curve given for mass ratio 3.31 was approximate, as explained above. Fully wetted theory is slightly conservative for mass ratios 2.29 and 3.31 whereas the 0.375 chord curve is unconservative for mass ratio 3.31. A 0.375-chord cavity length is representative of Cavitation Regime 1, as shown in Figure 5. This type of cavity did not occur during flutter runs made with mass ratio 1.44 because relatively high run speeds were selected in view of the high theoretical flutter speeds ($x_\alpha = 0.7$ was the maximum experimental value available). Experimental flutter frequencies are lower than those predicted by fully wetted flutter theory. Partially cavitating flutter theory for a 0.375-chord cavity, shown approximately for mass ratio 3.31 in Figure 10a, agrees more closely with the data.

In general, fully wetted flutter theory agrees fairly well with the experimental boundaries obtained for short cavities. The approximate theoretical results given for partially cavitating flutter theory indicate that the effects of this type of cavitation may be at least qualitatively described by the theory. However, a complete evaluation of the theory cannot be made on the basis of the limited amount of data and the incomplete theoretical calculations presented above. In an attempt to obtain additional experimental results for partially cavitating flow, the flutter test performed in the 24-in. water tunnel and described in the following section of this report was undertaken.

Supercavitating Hydrofoil Flutter

Flutter boundaries have been calculated using the two-dimensional, unsteady load expressions given by Woods[22] for supercavitating hydrofoils.

The cavity was assumed to be infinitely long ($\sigma = 0$) and to separate from the foil a distance 2bE aft of the leading edge. Loading for the fully wetted hydrofoil (E=1.0) is identical to Theodorsen loading. The flutter speed boundaries and frequency ratios are shown in Figures 11 and 12 for E = 0.0 (leading edge separation) and E = 0.05. If the E = 0.0 curves are extended to the x_α range of the data, the reduced flutter speeds are predicted to be about 0.2 for mass ratios 3.31 and 2.29 and about 0.5 for mass ratio 1.44. Therefore predictions for leading edge separation are over-conservative. The E = 0.05 curve was chosen to demonstrate that a small change in separation point near the leading edge of the foil brings the flutter speed into approximate agreement with the experimental values. This extreme sensitivity to separation point location is further illustrated in Figure 19. Unfortunately, the experimental separation point could not be observed and so a meaningful value of E cannot be drawn from test conditions. The separation point delay of 5 percent of the chord improves flutter frequency predictions for mass ratio 3.31, but worsens predictions for mass ratio 2.29. At reduced speeds below approximately 2.5, no theoretical flutter boundary was found to correspond to the flutter-free region above the experimental flutter boundary for $\mu = 3.31$, $x_\alpha = 0.438$.

Flutter experiments by Song[25] have indicated a tendency for the separation point of a long cavity from a sharp-edged foil to migrate downstream from the leading edge, possibly because of debris buildup. When leading edge separation was restored by cleaning the foil, the critical flutter speed was lowered. The foil was not cleaned during the present experiment. Another mechanism for delaying separation is the reattachment of flow a short distance aft of the leading edge after separation at the leading edge. This "turbulent bubble" effect occurs in fully wetted flow[17] but has not been reported for cavitating flow. It is concluded that a 5-percent separation delay may be reasonable for the semiwedge foil and that the experimental flutter points obtained do not necessarily disagree with predictions based on the Woods-Kaplan formulation. Verification of this theory, however, requires a study of separation point effects; such a

study is currently being conducted by Song, and preliminary results indicate at least qualitative agreement with the theory.*

CAVITY-INDUCED OSCILLATION TEST IN WATER TUNNEL

Following the towing basin flutter test described above, it was decided to make a more detailed survey of the effect of cavity length on flutter. Since cavity length could not be adequately controlled with the towing basin apparatus, a two-dimensional test section was constructed for use in the 24-in. variable-pressure water tunnel. The foil and foil suspension which had been tested in the towing basin were then installed in the water tunnel and flutter tested. The large amplitude oscillations that occurred have been identified as forced oscillations rather than classical flutter.

TWO-DIMENSIONAL TEST SECTION

A 27-in.-diameter semiclosed jet test section (Figure 20) was constructed for flutter testing in the 24-in. variable-pressure water tunnel. This test section had a conic transition to vertical walls which produced approximately two-dimensional flow over the hydrofoil. The two-degree-of-freedom foil suspensions were mounted on the outside of the vertical walls. Foil motions and pressures were monitored by strain and pressure gage outputs as described above. Plexiglass windows at the sides and top of the test section permitted visual observation of cavity size, but no photography was used.

EXPERIMENTAL PROCEDURE

The zero-speed angle of attack of the foil was set to 8.09 deg in order to produce a cavity at the leading edge. Pitching moment due to the flow caused the angle of attack to increase. At maximum speed, the angle of attack became 9.79 deg.

---

*Private communication.

Tunnel pressure was varied by changing the air pressure at the top of the tunnel above the free surface of the water. Water level was automatically maintained at a constant 3.42 ft above the centerline of the test section.

Various combinations of tunnel pressure and speed were used to produce cavities up to 3 chords in length, measured from the leading edge of the hydrofoil at the midspan position. Cavities longer than 3 chords would have extended beyond the test section walls.

VELOCITY CALIBRATION

Water speed was determined by correlating tunnel impeller rpm with a calibration curve obtained from pitot tube measurements inside the two-dimensional test section, as shown in Figure 20b. The pitot tube rake contained four total head tubes on one side and four static head tubes on the other side of the tunnel centerline; horizontal flow symmetry was assumed. All calibration measurements were made at atmospheric pressure above the free surface because other pressures could not be held constant during the reading of the manometer tubes.

The velocity calibration showed that the highest velocity occurred nearest the wall, with monotonically decreasing values toward the center. Since the highest and lowest velocities differed by no more than 1.8 percent on the average, the linear average of the four readings was taken as representative of section flow speed. Maximum tunnel speed obtained during calibration was 52.0 ft/sec, but the highest test run with the foil in place was made at 47.5 ft/sec because of loading limitations on the foil. Corrections for blockage effects were not considered necessary since the frontal areas of the foil and the pitot rake used for calibration were approximately equal.

CAVITATION CHARACTERISTICS

Cavities formed in the water tunnel did not exhibit the distant grouping by cavity length and pressure that characterized towing basin cavities. Instead, vapor cavities of continuously variable length were formed. All cavities showed some spanwise variation in length; only the midspan length was recorded. Cavities less than 1 chord in length were

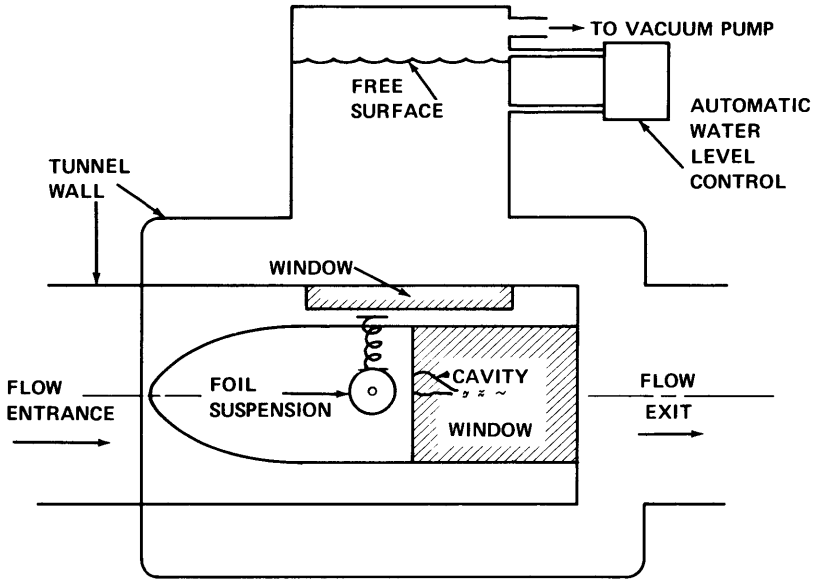

Figure 20a – Side View of Semiclosed Jet Test Section Installed

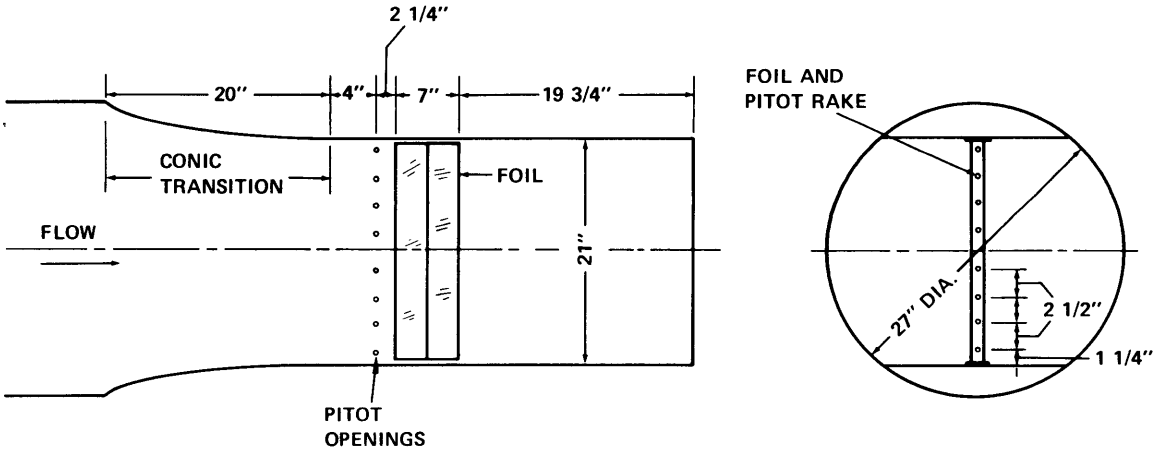

Figure 20b – Top and End Views of Hydrofoil Model Mounted in Test Section

Figure 20 – Semiclosed Jet Test Section of 24-Inch Variable Pressure Water Tunnel

observed from above the foil. Cavities longer than 1 chord were observed from below the foil where a clearly defined boundary was visible between the smooth cavity surface and the frothy wake region.

Cavities in the vicinity of 1 chord length were observed to oscillate in length as much as 0.25 chord. The cavity oscillations were accompanied by foil oscillations which are discussed below.

To illustrate the steady-state characteristics of the cavitating flow, cavitation number σ_v based on water vapor pressure has been plotted as a function of average cavity length in Figure 21. A few σ_c points are also plotted using cavity pressure data taken before the pressure gage failed. The lowest recorded pressure was 1.8 ft of water compared to 22.3 ft of water during towing basin testing; the lower pressure caused more severe pressure spiking when the cavity edge and wake passed over the pressure gage and may have contributed to gage failure. Figure 22 shows cavity length as a function of angle of attack divided by cavitation number, a relationship which is of theoretical interest. The angle of attack α' used in Figure 22 is referred to the zero-thickness chord line of the foil.

CAVITY-INDUCED OSCILLATION RESULTS

Three structural parameter configurations were tested in the water tunnel: x_α = 0.277, 0.403, and 0.553 for mass ratio 3.31. Because of limitations on foil load (due to the relatively high angle of attack) and tunnel pressure capability, all testing was performed within the reduced speed-cavity length region bounded by cross-hatched lines in Figure 23. Within this region, virtually all cavities between approximately 0.4 and 1.4 chords in length were accompanied by relatively large foil oscillations in both pitch and heave modes. The observed oscillation boundaries are shown by the dotted lines in Figure 23. For cavities longer or shorter than these boundaries, little or no unsteady foil motion was observed. The oscillation boundaries exhibited very little dependence on x_α, especially when experimental uncertainty is considered.

To determine the dependence of the foil oscillations on speed and cavity length, tunnel speed was held constant while cavity length was surveyed by varying tunnel pressure. Data for several water speeds were obtained in this way for each x_α.

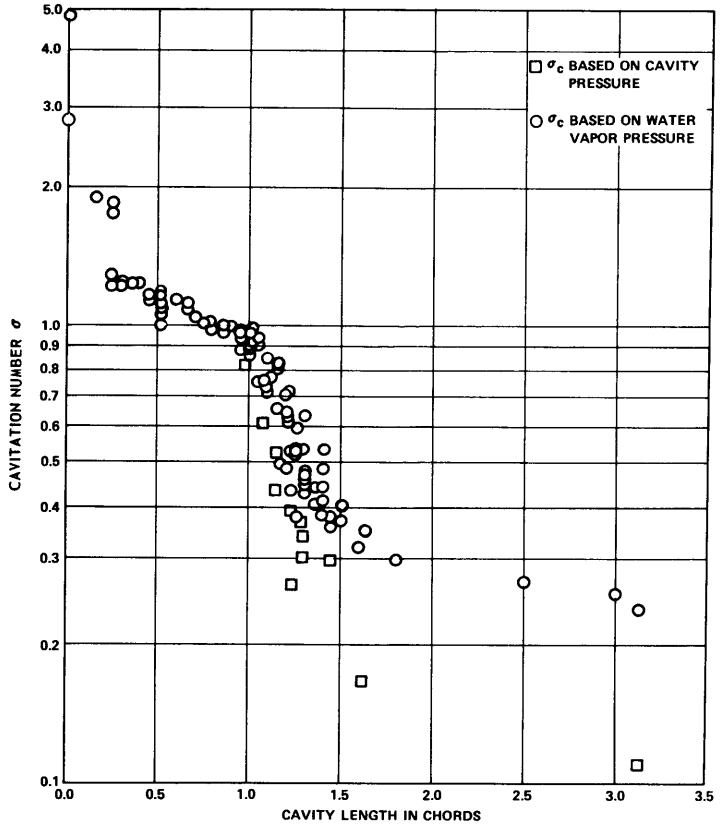

Figure 21 – Cavitation Number (σ) as a Function of Average Cavity Length for the Semiwedge Hydrofoil

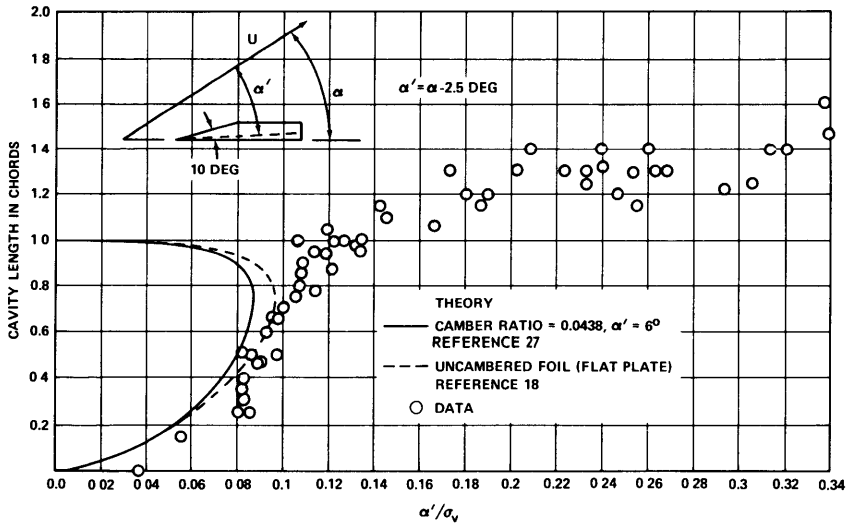

Figure 22 – Average Cavity Length as a Function of the Ratio of Zero-Thickness Angle of Attack (α') to Cavitation Number (σ_v) for the Semiwedge Hydrofoil

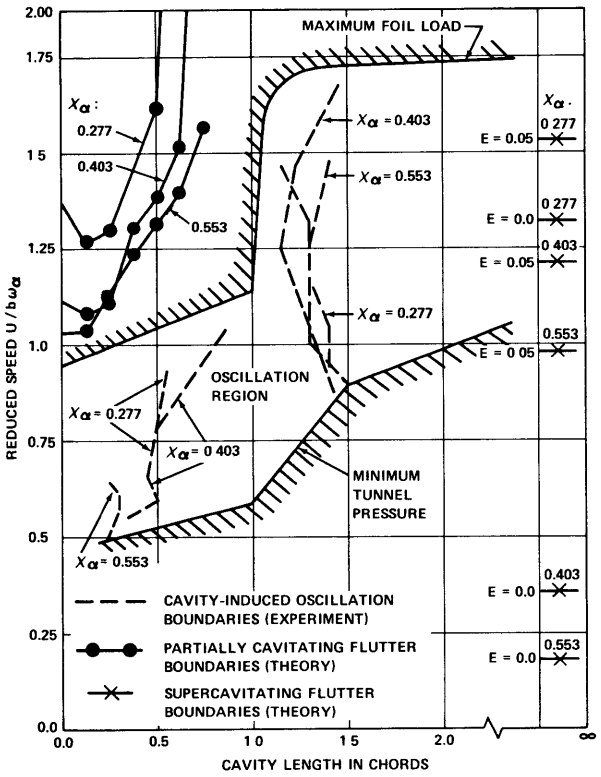

Figure 23 – Comparison of Experimental Oscillation Boundaries and Theoretical Flutter Boundaries

$\mu = 3.31$, $x_\alpha = 0.277, 0.403, 0.553$.

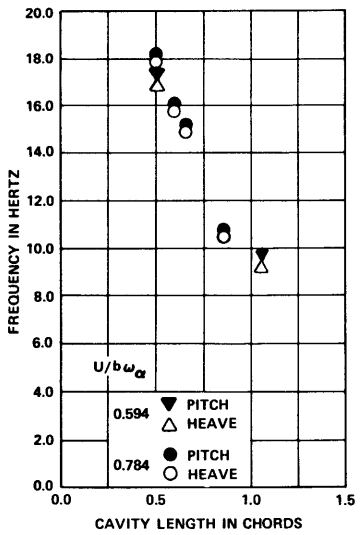

Figure 24a – $U/b\omega_\alpha = 0.594, 0.784$

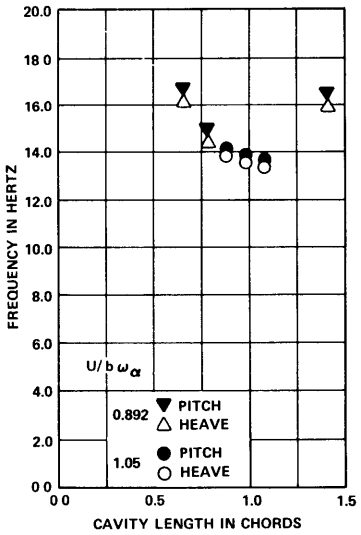

Figure 24b – $U/b\omega_\alpha = 0.892, 1.05$

Figure 24 – Cavity-Induced Oscillation Frequencies for Single-Frequency Oscillations as Functions of Cavity Length and Reduced Speed ($U/b\omega_\alpha$)

$\mu = 3.31$, $x_\alpha = 0.403$.

Marked changes in oscillation frequency occurred as cavity length was changed. Short cavity length oscillations displayed frequencies as high as 19.0 Hz. Frequency decreased as cavity length increased. Foil motion for cavities between 1.0 and 1.4 chords usually contained two or more frequency components. Oscillation frequencies for $x_\alpha = 0.403$ were determined by inspection of pen recordings and are plotted in Figure 24. Only single-frequency oscillations are represented since multiple-frequency oscillations corresponding to somewhat longer cavities could not be analyzed visually.

Since it became apparent during testing that a more accurate means of spectral analysis would be needed, foil motions for $x_\alpha = 0.277$ were recorded on magnetic tape. Subsequent spectral analysis by both analog and digital systems yielded the frequencies given in Figure 25; low intensity components are omitted. It is apparent that single-frequency oscillations occurred in both heave and pitch modes for cavities of 0.4 to approximately 1.0 chords, with frequencies decreasing as cavity length increased. For cavities between 1.0 and 1.4 chords, pitch and heave modes contained widely separated frequencies as well as common components. Frequencies in this multiple-frequency region often displayed harmonic relationships in both pitch and heave modes and between modes.

Amplitudes of oscillations were also strongly dependent on cavity length. Heave and pitch amplitudes are plotted against frequency in Figures 26 and 27. The amplitudes showed some dependence on velocity and exhibited one or more peaks which suggest resonance behavior. More data are needed to establish definite trends.

Phase analysis of foil motion for $x_\alpha = 0.277$ was made possible by digitization of tape-recorded runs on the Scientific Data System 910 Computer and subsequent Fourier analysis using IBM 7090 Computer programs. Relative phase angles between principal common frequency components of pitch and heave motions are plotted against frequency in Figure 28. The phase convention used in Figure 28 considers pitch and heave to be in phase when the positive coordinate maxima occur at the same time; positive coordinate directions are shown in Figure 3.

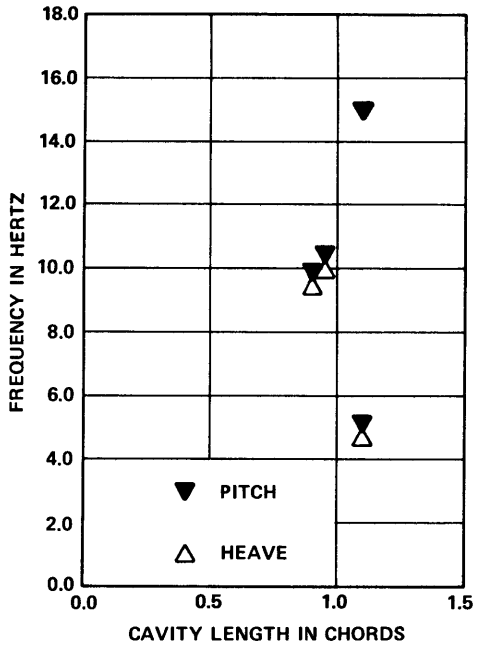

Figure 25a – $U/b\omega_\alpha = 0.665$

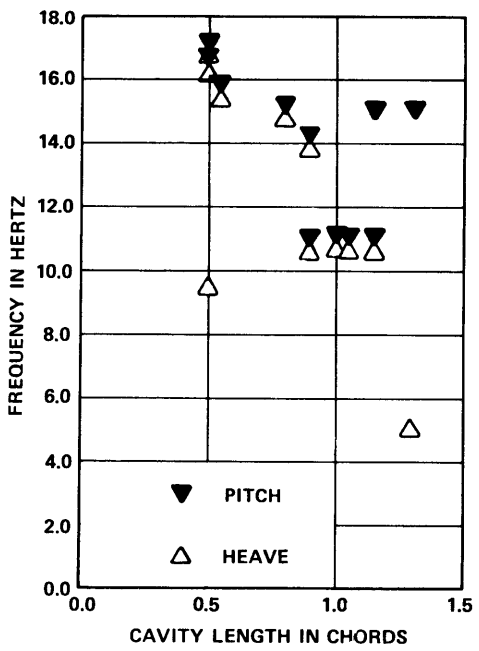

Figure 25b – $U/b\omega_\alpha = 0.784$

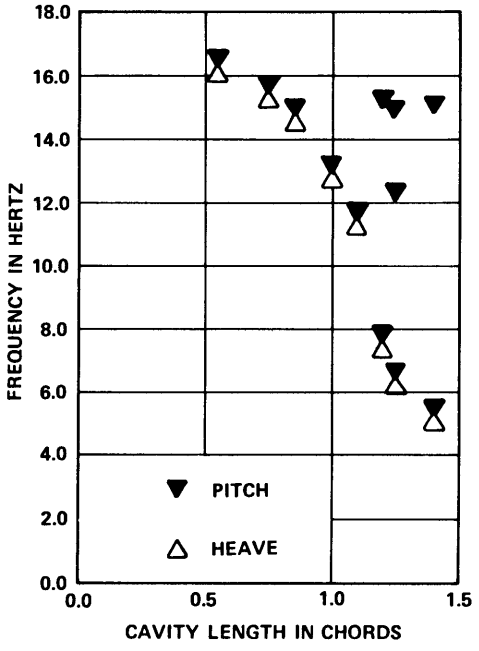

Figure 25c – $U/b\omega_\alpha = 0.910$

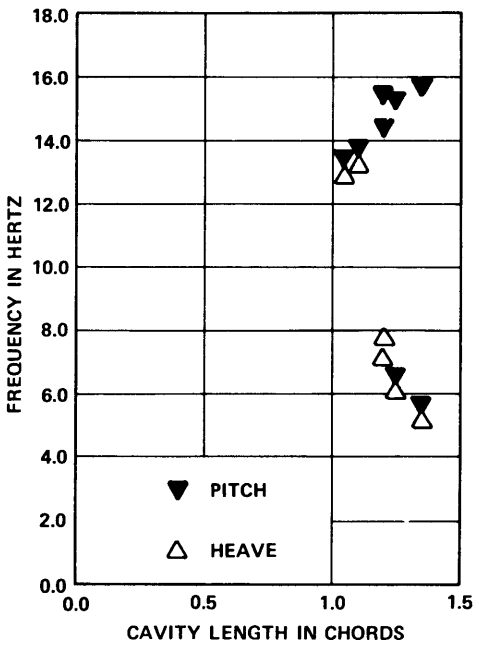

Figure 25d – $U/b\omega_\alpha = 1.05$

Figure 25 – Cavity-Induced Oscillation Frequencies for Single- and Multiple-Frequency Oscillations as Functions of Cavity Length and Reduced Speed ($U/b\omega_\alpha$)

$\mu = 3.31$, $x_\alpha = 0.277$.

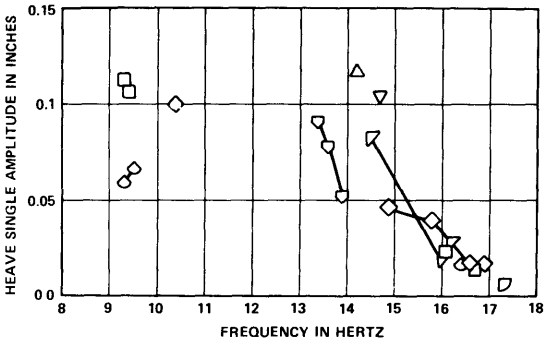

Figure 26a — Heave Amplitudes

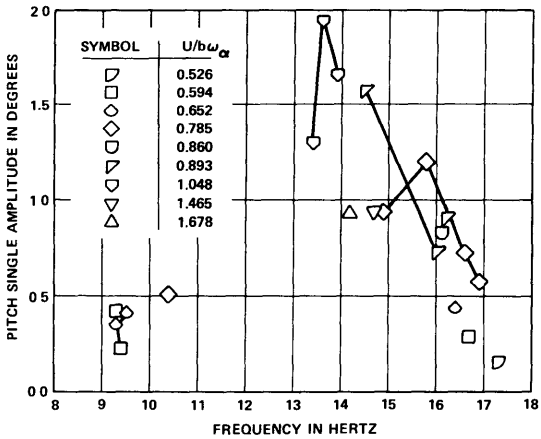

Figure 26b — Pitch Amplitudes

Figure 26 — Cavity-Induced Foil Oscillation Amplitudes for Single-Frequency Oscillations as Functions of Oscillation Frequency and Reduced Speed ($U/b\omega_\alpha$)

$\mu = 3.31$, $x_\alpha = 0.403$

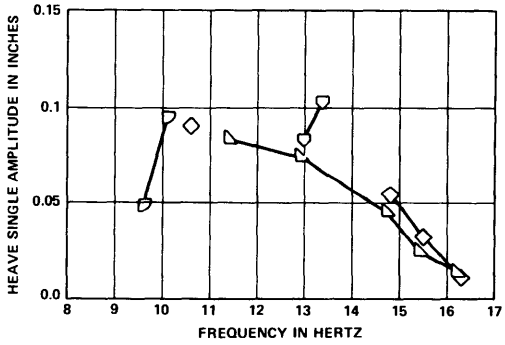

Figure 27a — Heave Amplitudes

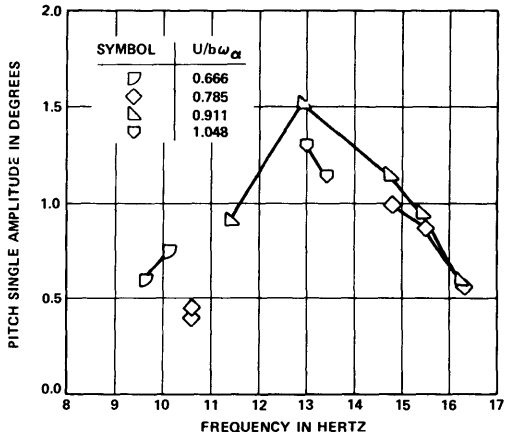

Figure 27b — Pitch Amplitudes

Figure 27 — Cavity-Induced Foil Oscillation Amplitudes for Single- and Multiple-Frequency Oscillations as Functions of Oscillation Frequency and Reduced Speed ($U/b\omega_\alpha$)

$\mu = 3.31$, $x_\alpha = 0.277$.

FORCED OSCILLATION ANALYSIS

The observed foil oscillations displayed boundaries which were substantially different from the flutter boundaries observed in the towing basin. Theoretical flutter boundaries for partially cavitating and supercavitating flow, which may be considered representative of flutter results obtained in the towing basin, are shown in Figure 23 along with the experimental oscillation boundaries. The foil oscillations occurred at much lower speeds than predicted for partially cavitating flutter. On the other hand, no oscillations occurred for relatively long cavities which might have approximated the infinite cavity region where supercavitating flutter would be expected. Therefore the possibility was considered that what was occurring was a cavity-induced forced oscillation rather than classical flutter. To provide a basis for determining whether the foil motion was a forced oscillation or flutter, an analysis[26] was made of the response of the foil suspension system to simple harmonic excitation in still water. The foil system was represented by Equations [1] with total mass $(m_h + m_\alpha)$ and moment of inertia I_α modified to include the added mass and moment of the foil. Free vibration resonances, calculated with zero loading, occur at 8.70 and 14.83 Hz.

When the pitch mode is driven by a sinusoidal moment and the heave mode remains free, the relative phase angle and the amplitudes of pitch and heave motion vary according to the driving frequency. At frequencies below 8.81 Hz, the uncoupled heave resonance, pitch leads heave by 180 deg whereas while above 8.81 Hz, pitch and heave are in phase. Pitch amplitude becomes zero at 8.81 Hz.

When the heave mode is driven and the pitch mode is free, pitch leads heave by 180 deg at frequencies below 14.31 Hz, the uncoupled pitch resonance. Above this, the two modes are in phase. Heave amplitude becomes zero at 14.31 Hz.

Phase angles for both types of forced oscillation are shown as a function of frequency by the dotted lines in Figure 28. Phase changes are more gradual when damping is present, as indicated by the rounded corners. Experimental data are also included in this figure.

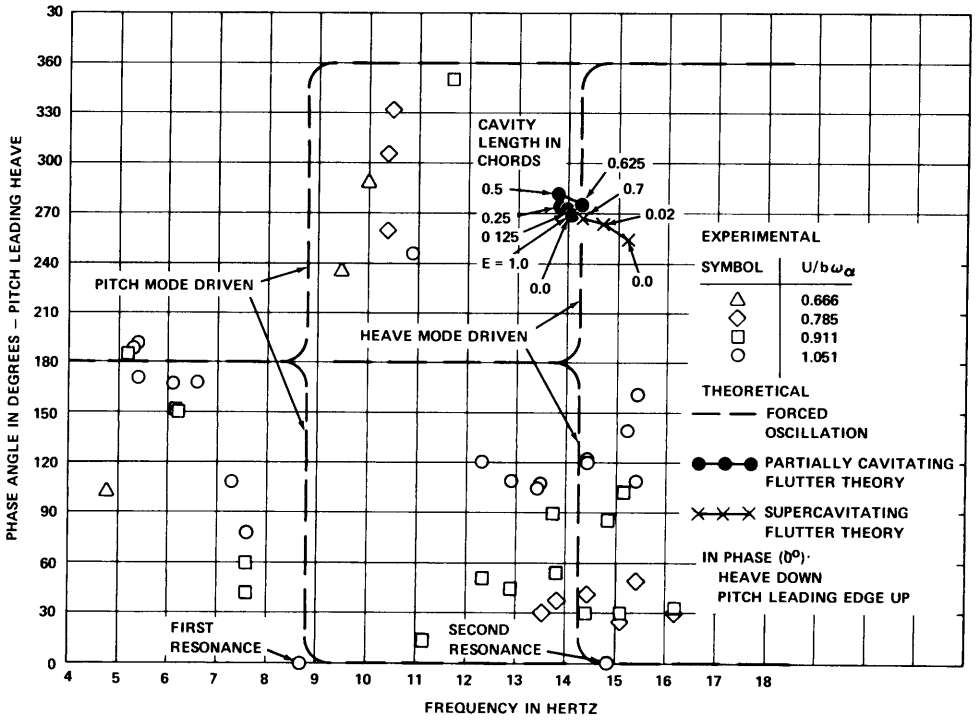

Figure 28 – Comparison of Experimental Phase Angles during Cavity-Induced Oscillations and Theoretical Phase Angles during Flutter and Forced Oscillation

$\mu = 3.31$, $x_\alpha = 0.277$.

DISCUSSION

Although the purpose of the water tunnel test was to obtain flutter data, several aspects of the observed foil oscillations did not resemble flutter. Flutter is a self-excited oscillation in which fluid and structure are coupled so as to produce negative damping; that is, energy flows from the fluid to the structure, resulting in oscillations of increasing amplitude. However, although the observed oscillation amplitudes were strongly dependent on cavity length, they remained well within the mechanical stops provided; for the most part, pitch amplitudes were substantially less than those observed during flutter in the towing basin. Flutter occurs within a speed range having well-defined boundaries; at speeds higher or lower than the boundaries, structural oscillations are negatively damped. In contrast, the observed oscillations did not exhibit a speed boundary within the speed range tested, but rather the oscillations occurred at all speeds when cavity length was between 0.4 and 1.4 chords. Flutter oscillations are characterized by a single frequency in all structural modes that are coupled, whereas the observed oscillations often displayed multiple frequencies in pitch and heave modes for cavities between 1.0 and 1.4 chords. On a more quantitative basis, it has already been mentioned that the oscillation boundaries showed no similarity with flutter boundaries obtained during the towing basin test.

By using the two cavitating flutter theories described above, one can calculate the relative phase angles between pitch and heave motion that should characterize flutter in partially cavitating and supercavitating flow. These phase angles are plotted as a function of flutter frequency in Figure 28, along with experimental phase angles as a function of oscillation frequency. The predicted phase angles for flutter were between 255 and 282 deg; experimental phase angles in the same frequency region fell between 25 and 160 deg.

The failure of the observed oscillations to exhibit any of the above-described qualitative or quantitative flutter characteristics is a strong indication that flutter did not occur. However, all of the observed results would be expected if the foil had been driven in forced oscillation by unsteady cavity effects. The presence of oscillations and the

oscillation frequency would depend on cavity structure, perhaps to a greater extent than on water speed. Foil amplitudes would exhibit resonance behavior, and oscillations would not be limited to a single frequency. The data indicate that cavity length rather than water speed was the principal parameter that affected the oscillations. There was good agreement between experimental phase angles and the phase angles calculated for forced oscillation, but flutter phase angles had no values in common with the data. This agreement occurred even though the experimental phase angles were obtained during test runs when flow velocity would be expected to influence coupling between pitch and heave, especially if a flutter boundary were near. It is therefore concluded that what occurred was a forced oscillation rather than flutter.

Some idea about the nature of the cavity-induced excitation may be obtained from the frequency data in Figure 25. In the cavity length region from 0.4 to 1.0 chords, oscillation frequency decreased as the cavity length increased. This relationship suggests that wave motion along the walls of the cavity may have been involved. For cavities of 1.0 to 1.4 chords, a similar trend occurred in the lower frequency branch; this may have been a continuation of the frequency curve for shorter cavities. The other frequencies which appeared in the multiple-frequency region were either harmonics of the lowest frequency or close to 15 Hz, the approximate higher resonance of the submerged foil system. Thus a wide-band excitation effect may have been produced by the longer cavities.

The existence of an instability in cavity length is supported by steady-load calculations of Guerst[18] and of Guerst and Verbrugh.[27] The predicted relationship for steady angle of attack α' (referred to the zero-thickness foil), cavitation number (σ_v is used to approximate σ_c), and cavity length is shown in Figure 22 for an uncambered foil and a cambered foil which simulated the mean line of the semiwedge foil. The double-valued cavity length function, along with other theoretical considerations discussed in Reference 18, implies an instability for cavities longer than 0.75 chord. The cavity oscillations of Kermeen,[15] Meijer,[16] Wade,[17] and the present experiment apparently correspond to this instability. It might be noted that Steinberg and Karp[20] derived their load theory by considering the unsteady loading as an oscillation about the steady loading of Guerst. The steady loading agreed well with data for cavities of less than 0.75 chord.

CONCLUSIONS

During the towing basin experiment, flutter was obtained for short (less than 0.5 chord) vapor-filled cavities and for very long (several chords) ventilated cavities. Uncertainties in cavity length for the short cavities and in separation point for the long cavities prevent making an exact comparison of the data with theoretical predictions. Such a comparison is further hindered by the known inaccuracy in the partially cavitating flutter theory which was used. It is felt, however, that within the limits of theory and experiment, the experimental flutter results do not disagree with the theoretical predictions of partially cavitating and supercavitating flutter theory. In particular, the dependence of flutter speed and frequency on mass unbalance x_α is in good agreement with the theoretical trend.

In both testing facilities, a region of intermediate cavity length was encountered in which classical flutter did not occur. Part of this region was characterized by the presence of cavity-induced foil oscillations which, unlike flutter, have been identified as positively damped forced oscillations. The remainder of the region exhibited no oscillations of observable amplitude. It is possible that the cavity length region in which flutter did not occur corresponds to the flutter-free region predicted by partially cavitating flutter theory for cavities longer than 0.75 chord. However, the absence of flutter for 1- and 2-chord cavities in the towing basin may have been due to the limited speed ranges and structural parameter values for which these cavities were tested. Similarly, although no flutter was observed in the water tunnel for cavities between 1 and 3 chords at relatively high speeds, this region cannot be considered free of flutter until it has been demonstrated that flutter can occur in the facility.

It is therefore concluded that although the present data do not disagree with the predictions of flutter theory, they are insufficient to confirm the theory for practical use. In addition, the partially cavitating flutter theory is inadequately defined by the published coefficients for comparison with experimental results.

The foil oscillations obtained for cavities between 0.4 and 1.4 chords during testing in the water tunnel are concluded to have been forced oscillations caused by unsteady cavity effects. The relative phase angle between pitch and heave motion was found to be a suitable quantity for distinguishing between flutter and cavity-induced oscillation. The oscillation which occurred for 1-chord cavities in the towing basin may have been cavity-induced oscillation, but this cannot be positively identified because phase angles could not be obtained. It appears that the unsteady cavity effects are related to the double-valued cavity length function predicted by the partially cavitating load theory of Guerst.

RECOMMENDATIONS

PARTIALLY CAVITATING FLUTTER

A meaningful study of partially cavitating flutter in two-dimensional flow requires a more complete table of load coefficients than is now available in Reference 20. Additional experimental data in which cavity length is surveyed are also needed.

The following recommendations are made:

1. Additional load coefficients for partially cavitating hydrofoils should be calculated from the expressions given in Reference 28 so that accurate theoretical flutter predictions can be made.
2. A parametric study of flutter boundaries should be made using the expanded table of load coefficients. This study should determine the feasibility of additional experimental testing.
3. If additional flutter tests appear feasible, they should be made. The testing should be performed in the water tunnel to permit cavity length to be surveyed. In order to reduce loading, a new hydrofoil model which will permit partial cavitation from the leading edge at low angles of attack may be required.
4. A flutter study of a three-dimensional hydrofoil should be made using two-dimensional partially cavitating load theory combined with a modal representation of the structure. This study should indicate the effect of partial cavitation on the flutter characteristics of a practical hydrofoil. Experiments should be conducted to confirm predicted effects.

SUPERCAVITATING FLUTTER

Theoretical calculations indicate a substantial lowering of flutter speeds when leading edge separation occurs. Further experimental verification of the theory is required; this is currently being carried out by Song. If experimental verification is obtained, it is recommended that a flutter study of a three-dimensional hydrofoil be made using two-dimensional supercavitating load theory combined with a modal representation of the structure. This study should indicate the effect of very long cavities on the flutter characteristics of a practical hydrofoil. Experiments should be conducted to confirm predicted results.

CAVITY-INDUCED OSCILLATION

Unsteady loading occurs when cavities between 0.4 and 1.4 chords in length are present. The results of the present experiment indicate that, unlike flutter, the effect is independent of speed and is positively damped. Excitation of structural components by this phenomenon could lead to structural fatigue. Hydrofoil flutter characteristics in this cavity regime remain to be determined. The following recommendations are made:

1. Existing cavitating hydrofoil data, such as those obtained from surface-piercing strut tests, should be examined for further evidence of unsteady cavity effects.

2. Theoretical and experimental studies should be made to determine the mechanism of cavity oscillation so that its effects on full-scale hydrofoils can be predicted. In particular, the relationship between the cavity-induced loading and the structural response of the hydrofoil should be determined.

ACKNOWLEDGMENTS

The author gratefully acknowledges the advice, assistance, and encouragement given by Mr. Daniel S. Cieslowski in all phases of the present work. Mr. Cieslowski also directed the towing basin test. The contributions of Dr. C.S. Song, who offered many helpful suggestions and acted as an observer during the water tunnel test while on leave from the University of Minnesota, are also appreciated. Design of the foil suspension

was based on a suggestion made by Dr. Charles J. Henry of the Davidson Laboratory, Stevens Institute of Technology, in a conversation with Dr. David A. Jewell of this Center.

Additional contributions were made by several NSRDC personnel including Miss Lorraine R. Dutcher who performed a digital spectral analysis of the tape-recorded data, Mr. Irvin L. Young who performed an analog spectral analysis of the same data, Mr. George W. Gilbert who designed the two-dimensional test section which was used in the water tunnel, and Mr. Mills Dean who designed and constructed the pressure gage mounted in the top surface of the foil.

REFERENCES

1. McGoldrick, R.T., "Rudder-Excited Hull Vibration on USS FORREST SHERMAN (DD 931) (A Problem in Hydroelasticity)," Transactions, Society of Naval Architects and Marine Engineers, Vol. 67, pp. 341-385 (1959). Also David Taylor Model Basin Report 1431 (Jun 1960).

2. Jewell, D.A. and McCormick, M.E., "Hydroelastic Instability of a Control Surface," David Taylor Model Basin Report 1442 (Dec 1961).

3. Baird, E.F. et al., "An Experimental and Theoretical Investigation of Hydrofoil Flutter," Aerospace Engineering, Vol. 21, No. 2, pp. 34-41 (Feb 1962).

4. Squires, C.E., Jr. and Baird, E.F., "The Flutter Characteristics of a Hydrofoil Strut," Proceedings Fourth Naval Hydrodynamics Symposium (Aug 1962).

5. Caporali, R.L. and Brunelle, E.J., "Hydrofoil Instability at Low Mass Density Ratios," Princeton University, Aerospace and Mechanical Sciences Report 670 (Mar 1964).

6. Abramson, H.N. and Ransleben, G.E., Jr., "An Experimental Investigation of Flutter of a Fully Submerged Subcavitating Hydrofoil," Southwest Research Institute, Contract Nonr-3335(00) (Dec 1963).

7. Abramson, H.N. and Langner, C.G., "Correlation of Various Subcavitating Hydrofoil Flutter Predictions Using Modified Oscillatory Lift and Moment Coefficients," Southwest Research Institute, Contract NObs-88599 (Jun 1964).

8. Yates, E.C., Jr., "Flutter Prediction at Low Mass-Density Ratios with Application to the Finite-Span Noncavitating Hydrofoil," AIAA Third Marine Systems and ASW Meeting (Apr-May 1968).

9. Rowe, W.S. and Marvin, T.G.B., "A Program of Theoretical Research on Hydroelastic Stability," The Boeing Company, Contract N00014-67-C-0248 (Nov 1968).

10. Henry, C.J., "Comparison of Hydrofoil Flutter Phenomenon and Airfoil Flutter Theory," Proceedings Fourth Naval Hydrodynamics Symposium (Aug 1962).

11. Cieslowski, D.S. and Pattison, J.H., "Unsteady Hydrodynamic Loads and Flutter of Two-Dimensional Hydrofoils," Spring Meeting Hydrofoil Symposium, Society of Naval Architects and Marine Engineers, Paper 2-b (May 1965).

12. Theodorsen, T., "General Theory of Aerodynamic Instability and the Mechanism of Flutter," NACA Report 496 (1935).

13. Theodorsen, T. and Garrick, I.E., "Mechanism of Flutter: A Theoretical and Experimental Investigation of the Flutter Problem," NACA Report 685 (1940).

14. Bisplinghoff, R.L. et al., "Aeroelasticity," Addison-Wesley Publishing Company, Cambridge, Massachusetts (1955), p. 533.

15. Kermeen, R.W., "Water Tunnel Tests of NACA 4412 and Walchner Profile 7 Hydrofoils in Noncavitating and Cavitating Flows," California Institute of Technology Hydrodynamics Laboratory Report 47-5 (Feb 1956).

16. Meijer, M.C., "Some Experiments on Partially Cavitating Hydrofoils," International Shipbuilding Progress, Vol. 6, No. 60, pp. 361-368 (Aug 1959).

17. Wade, R.B., "Water Tunnel Observations on the Flow Past a Plano-Convex Hydrofoil," California Institute of Technology, Division of Engineering and Applied Science Report E-79-6 (Feb 1964).

18. Guerst, J.A., "Linearized Theory for Partially Cavitated Hydrofoils," International Shipbuilding Progress, Vol. 6, No. 60, pp. 369-384 (Aug 1959).

19. Brownell, W.F. and Miller, M.L., "Hydromechanics Cavitation Research Facilities and Techniques in Use at the David Taylor Model Basin," Symposium on Cavitation Research Facilities and Techniques, American Society of Mechanical Engineers (May 1964); also David Taylor Model Basin Report 1856 (Oct 1964).

20. Steinberg, H. and Karp, S., "Unsteady Flow past Partially Cavitated Hydrofoils," Proceedings Fourth Naval Hydrodynamics Symposium (Aug 1962).

21. Kaplan, P., "Hydroelastic Instabilities of Partially Cavitated Hydrofoils," Proceedings Fourth Naval Hydrodynamics Symposium (Aug 1962).

22. Woods, L.C., "Aerodynamic Forces on an Oscillating Aerofoil Fitted with a Spoiler," Proceedings of the Royal Society of London, Series A, Vol. 239, pp. 328-337 (1957).

23. Kaplan, P. and Henry, C.J., "A Study of the Hydroelastic Instabilities of Supercavitating Hydrofoils," Journal of Ship Research, Vol. 4, No. 3, pp. 28-38 (Dec 1960).

24. Patton, J. and Borden, A., "Computation of Oscillatory Loads on a Supercavitating Hydrofoil," David Taylor Model Basin Report 1840 (Aug 1965).

25. Song, C.S. and Almo, J., "An Experimental Study of the Hydroelastic Instability of Supercavitating Hydrofoils," University of Minnesota, St. Anthony Falls Hydraulic Laboratory Project Report 89 (Feb 1967).

26. Morse, P.M., "Vibration and Sound," Second Edition, McGraw-Hill Book Company, New York (1948), pp. 52-66.

27. Guerst, J.A. and Verbrugh, P.J., "A Note on Camber Effects of a Partially Cavitated Hydrofoil," International Shipbuilding Progress, Vol. 6, No. 61, pp. 409-414 (Sep 1959).

28. Steinberg, H., "Linearized Theory of the Unsteady Motion of a Partially Cavitated Hydrofoil," TRG Report TRG-153-SR-1 (Mar 1962).

INITIAL DISTRIBUTION

Copies	
4	NAVSHIPSYSCOM 1 Ships 0342 2 Ships 2052 1 Ships 03412
3	ONR 2 Code 438 1 Code 411
1	ONR Boston
1	ONR Chicago
1	Onr New York
1	ONR Pasadena
1	ONR San Francisco
1	ONR London
3	NAVSEC 1 SEC 6132 1 SEC 6136 1 SEC 6140
1	NAVFACENGCOM
1	SPECPROJO Attn: Dr. John Craven (NSP-001)
1	CO NAVAIRDEVCEN
1	NASL
1	NRL (Code 2027)
1	NAVUWRES
1	NAVOCEANO
1	Commander U.S. Naval Proving Ground Dahlgren, Va 22448 Attn: Tech Lib
1	CIVENGRLAB Attn: Code L31
1	NAVSHIPYD BSN
1	NAVSHIPYD CHASN
1	NAVSHIPYD NORVA
1	NAVSHIPYD PHILA
1	NAVSHIPYD PTSMH
1	NAVSHIPYD BREM Attn: Engr Lib Code 245.6

Copies	
1	AFFDL (FDDS - Mr. J. Olsen) Wright-Patterson AFB, Ohio 45433
1	NASA Scientific & Technical Information Facility P.O. Box 33 College Park, Md 20740
1	Library of Congress Sci & Technology Div
1	COGARD Attn: Div of Merchant Marine Safety
1	Director Waterways Experiment Station Box 631 Vicksburg, Mississippi 39180 Attn: Research Center Lib
1	Univ of Bridgeport Bridgeport, Connecticut 06602 Attn: Prof. Earl Uram Mechanical Engr Dept
4	Naval Architecture Dept College of Engr Univ of California Berkeley, Calif 94720 Attn: 1 Lib 1 Prof J.R. Paulling 1 Prof. J.V. Wehausen 1 Dr. H.A. Schade
1	NASA Langley Attn: Dr. E.C. Yates, Jr., MS 340
3	CIT, Pasadena Attn: 1 Dr. A.J. Acosta 1 Dr. T.Y. Wu 1 Dr. M.S. Plesset
1	Univ of Connecticut Box U-37 Storrs, Connecticut 06268 Attn: Prof. V. Scottron Hydraulic Research Lab
1	Cornell Univ Graduate School of Aerospace Engr. Ithaca, New York 14850 Attn: Prof. W.R. Sears

Copies	
1	Harvard Univ. 2 Divinity Avenue Cambridge, Mass 02138 Attn: Prof. G. Birkhoff Dept of Mathematics
1	Univ of Illinois College of Engr Urbana, Illinois 61801 Attn: Dr. J.M. Robertson Theoretical & Applied Mechanics Dept
1	The Univ of Iowa Iowa City, Iowa 52240 Attn: Dr. Hunter Rouse
2	The State Univ of Iowa Iowa Inst of Hydraulic Research Iowa City, Iowa 52240 Attn: 1 Dr. L. Landweber 1 Dr. J. Kennedy
1	Kansas State Univ Engineering Experiment Station Seaton Hall Manhattan, Kansas 66502 Attn: Prof. D.A. Nesmith
1	Lehigh University Bethlehem, Pa 18015 Attn: Fritz Lab Lib
7	MIT, Hydro Lab Cambridge Attn: Prof. A.T. Ippen
6	MIT, Dept NAME Attn: 1 Dr. A.H. Keil, Rm 5-226 1 Prof. P. Mandel, Rm 5-325 1 Prof. J.R. Kerwin, Rm 5-23 1 Prof. P. Leehey, Rm 5-222 1 Prof. M. Abkowitz 1 Dr. J.N. Newman
2	Univ of Michigan, Dept of NAME Ann Arbor Attn: 1 Dr. T.F. Ogilvie 1 Prof. H. Benford
5	St. Anthony Falls Hydraulic Lab Univ of Minnesota Mississippi River at 3rd Ave S.E. Minneapolis, Minnesota 55414 Attn: 1 Dir 1 Dr. C.S. Song 1 Mr. J.M. Killen 1 Mr. F. Schiebe 1 Mr. J.M. Wetzel
1	USNA
1	USNAVPGSCHOL
1	New York Univ Univ Heights Bronx, New York 10453 Attn: Prof. W.J. Pierson, Jr.
2	New York Univ Courant Inst of Mathe Sci 251 Mercier St New York, New York 10012 Attn: 1 Prof. A.S. Peters 1 Prof. J.J. Stoker
1	Univ of Notre Dame Notre Dame, Indiana 46556 Attn: Dr. A.F. Strandhagen
2	The Pennsylvania State Univ Ordnance Research Lab Univ Park, Pa 16801 Attn: 1 Director 1 Dr. G. Wislicenus
3	Stanford Univ, Stanford, Calif 94305 Attn: 1 Prof. H. Ashley Dept of Aeronautics & Astronautics 1 Prof. R.L. Street Dept of Civil Engr 1 Prof. B. Perry Dept of Civil Engr
3	SIT, DL Attn: Dr. J. Breslin
1	Worcester Polytechnic Inst Alden Research Labs Worcester, Mass 01609 Attn: Director

Copies

1 Aerojet-General Corp
1100 W. Hollyvale St
Azusa, Calif 91702
Attn: Mr. J. Levy
Bldg 160, Dept 4223

1 Bethlehem Steel Corp
Central Technical Div
Sparrows Point Yard
Sparrows Point, Md 21219
Attn: Mr. A.D. Haff
Technical Manager

1 Bethelhem Steel Corp
25 Broadway
New York, N.Y. 10004
Attn: Mr. H. deLuce

7 The Boeing Co, Aerospace Grp
Advanced Marine Systems
P.O. Box 3707
Seattle, Washington 98124
Attn: 1 Mr. R.R. Barbar
Lib Unit Chief
1 Mr. H. French
1 Mr. R. Hatte
1 Mr. R. Hubard
1 Mr. F.B. Watson
1 Mr. W.S. Rowe
1 Mr. T.G.B. Marvin

1 Cornell Aeronautical Lab
Applied Mechanics Dept
P.O. Box 235
Buffalo, New York 14221
Attn: Dr. I.C. Statler

1 Electric Boat Div
General Dynamics Corp
Groton, Connecticut 06340
Attn: Mr. V.T. Boatwright, Jr.

1 General Applied Sci Labs, Inc.
Merrick & Stewart Avenues
Westbury, L.I., N.Y. 11590
Attn: Dr. F. Lane

1 Gibbs & Cox, Inc.
21 West Street
New York, N.Y. 10006
Attn: Techn Infor Control Sec

1 Grumman Aircraft Engr Corp
Bethpage, L.I., N.Y. 11714
Attn: Mr. W.P. Carl

Copies

2 Hydronautics, Incorporated
Pindell School Road
Howard County
Laurel, Md 20810
Attn: 1 Mr. P. Eisenberg
1 Mr. M.P. Tulin

1 Nat'l Sci Foundation
Engr Division
1800 G Street, N.W.
Washington, D.C. 20550
Attn: Director

1 Newport News Shipbuilding
& Drydock Co
4101 Washington Avenue
Newport News, Va 23607
Attn: Techn Lib Dept

1 Oceanics, Incorporated
Technical Industrial Park
Plainview, L.I.,
New York 11803
Attn: Dr. Paul Kaplan

1 Robert Taggart, Inc
3930 Walnut Street
Fairfax, Va 22030
Attn: Mr. R. Taggart

1 Sperry-Piedmont Co
Charlottesville, Va 22901
Attn: Mr. T. Noble

UNCLASSIFIED

Security Classification

DOCUMENT CONTROL DATA - R & D

(Security classification of title, body of abstract and indexing annotation must be entered when the overall report is classified)

1 ORIGINATING ACTIVITY (Corporate author)	2a. REPORT SECURITY CLASSIFICATION
Naval Ship Research and Development Center Washington, D.C. 20007	UNCLASSIFIED
	2b. GROUP

3 REPORT TITLE

FLUTTER AND CAVITY-INDUCED OSCILLATION OF A TWO-DEGREE-OF-FREEDOM HYDROFOIL IN TWO-DIMENSIONAL CAVITATING FLOW

4 DESCRIPTIVE NOTES (Type of report and inclusive dates)

Final Report

5 AUTHOR(S) (First name, middle initial, last name)

Peter K. Besch

6 REPORT DATE	7a. TOTAL NO. OF PAGES	7b. NO OF REFS
April 1969	64	28

8a. CONTRACT OR GRANT NO.	9a. ORIGINATOR'S REPORT NUMBER(S)
SS 46-06	
b. PROJECT NO.	3000
c.	9b. OTHER REPORT NO(S) (Any other numbers that may be assigned this report)
d. Task 1703	

10 DISTRIBUTION STATEMENT

This document has been approved for public release and sale; its distribution is unlimited.

11. SUPPLEMENTARY NOTES	12. SPONSORING MILITARY ACTIVITY

13. ABSTRACT

Two hydrofoil flutter tests were performed at the Naval Ship Research and Development Center using a two-degree-of-freedom, semiwedge hydrofoil in two-dimensional cavitating flow. In the first test, conducted in the high-speed towing basin, four distinct cavity lengths were tested. Flutter occurred for cavities 1/2 and several chords in length. Cavity-induced oscillations may have occurred for 1-chord cavities, but no oscillations were observed for 2-chord cavities. The flutter results are compared with flutter boundaries predicted by partially cavitating and supercavitating flutter theories. It is concluded that the experimental flutter results do not disagree with the predicted values.

In the second test, conducted in the 24-in. variable-pressure water tunnel, cavity lengths were varied from 0 to 3 chords. Cavity-induced oscillations were observed for cavities between 0.4 and 1.4 chords in length, but other cavity lengths were free of oscillation. The oscillations are discussed in terms of forced oscillations of a coupled two-degree-of-freedom elastic system. It is concluded that the cavity-induced oscillations, unlike flutter, are positively damped oscillations. Several recommendations are given for further experimental and theoretical studies.

14 KEY WORDS	LINK A		LINK B		LINK C	
	ROLE	WT	ROLE	WT	ROLE	WT
Flutter						
Oscillation (Cavity-Induced)						
Partially Cavitating Hydrofoils						
Supercavitating Hydrofoils						
Towing Basin Testing						
Ventilation						
Water Tunnel Testing						

Naval Ship R&D Center. Report 3000.
FLUTTER AND CAVITY-INDUCED OSCILLATION OF A TWO-DEGREE-OF-FREEDOM HYDROFOIL IN TWO-DIMENSIONAL CAVITATING FLOW, by Peter K. Besch. Apr 1969. vii, 57p. illus., refs. UNCLASSIFIED

Two hydrofoil flutter tests were performed at the Naval Ship Research and Development Center using a two-degree-of-freedom, semiwedge hydrofoil in two-dimensional cavitating flow. In the first test, conducted in the high-speed towing basin, four distinct cavity lengths were tested. Flutter occurred for cavities 1/2 and several chords in length. Cavity-induced oscillations may have occurred for 1-chord cavities, but no oscillations were observed for 2-chord cavities. The flutter results are compared with flutter boundaries predicted by partially cavitating and supercavitating flutter theories. It is

1. Supercavitating hydrofoils--Ventilation--Flutter--Towing basin tests
2. Partially cavitating hydrofoils--Flutter--Towing basin tests
3. Supercavitating hydrofoils--Oscillation (Cavity-induced)--Water-tunnel tests
4. Partially cavitating hydrofoils--Oscillation (Cavity induced)--Water-tunnel tests

Naval Ship R&D Center. Report 3000.
FLUTTER AND CAVITY-INDUCED OSCILLATION OF A TWO-DEGREE-OF-FREEDOM HYDROFOIL IN TWO-DIMENSIONAL CAVITATING FLOW, by Peter K. Besch. Apr 1969. vii, 57p. illus., refs. UNCLASSIFIED

Two hydrofoil flutter tests were performed at the Naval Ship Research and Development Center using a two-degree-of-freedom, semiwedge hydrofoil in two-dimensional cavitating flow. In the first test, conducted in the high-speed towing basin, four distinct cavity lengths were tested. Flutter occurred for cavities 1/2 and several chords in length. Cavity-induced oscillations may have occurred for 1-chord cavities, but no oscillations were observed for 2-chord cavities. The flutter results are compared with flutter boundaries predicted by partially cavitating and supercavitating flutter theories. It is

1. Supercavitating hydrofoils--Ventilation--Flutter--Towing basin tests
2. Partially cavitating hydrofoils--Flutter--Towing basin tests
3. Supercavitating hydrofoils--Oscillation (Cavity-induced)--Water-tunnel tests
4. Partially cavitating hydrofoils--Oscillation (Cavity induced)--Water-tunnel tests

concluded that the experimental flutter results do not disagree with the predicted values.
In the second test, conducted in the 24-in. variable-pressure water tunnel, cavity lengths were varied from 0 to 3 chords. Cavity-induced oscillations were observed for cavities between 0.4 and 1.4 chords in length, but other cavity lengths were free of oscillation. The oscillations are discussed in terms of forced oscillations of a coupled two-degree-of-freedom elastic system. It is concluded that the cavity-induced oscillations, unlike flutter, are positively damped oscillations. Several recommendations are given for further experimental and theoretical studies.

I. Besch, Peter K.

concluded that the experimental flutter results do not disagree with the predicted values.
In the second test, conducted in the 24-in. variable-pressure water tunnel, cavity lengths were varied from 0 to 3 chords. Cavity-induced oscillations were observed for cavities between 0.4 and 1.4 chords in length, but other cavity lengths were free of oscillation. The oscillations are discussed in terms of forced oscillations of a coupled two-degree-of-freedom elastic system. It is concluded that the cavity-induced oscillations, unlike flutter, are positively damped oscillations. Several recommendations are given for further experimental and theoretical studies.

I. Besch, Peter K.

Naval Ship R&D Center. Report 3000.
FLUTTER AND CAVITY-INDUCED OSCILLATION OF A TWO-DEGREE-OF-FREEDOM HYDROFOIL IN TWO-DIMENSIONAL CAVITATING FLOW, by Peter K. Besch. Apr 1969. vii, 57p. illus., refs. UNCLASSIFIED

Two hydrofoil flutter tests were performed at the Naval Ship Research and Development Center using a two-degree-of-freedom, semiwedge hydrofoil in two-dimensional cavitating flow. In the first test, conducted in the high-speed towing basin, four distinct cavity lengths were tested. Flutter occurred for cavities 1/2 and several chords in length. Cavity-induced oscillations may have occurred for 1-chord cavities, but no oscillations were observed for 2-chord cavities. The flutter results are compared with flutter boundaries predicted by partially cavitating and supercavitating flutter theories. It is concluded that the experimental flutter results do not disagree with the predicted values.

In the second test, conducted in the 24-in. variable-pressure water tunnel, cavity lengths were varied from 0 to 3 chords. Cavity-induced oscillations were observed for cavities between 0.4 and 1.4 chords in length, but other cavity lengths were free of oscillation. The oscillations are discussed in terms of forced oscillations of a coupled two-degree-of-freedom elastic system. It is concluded that the cavity-induced oscillations, unlike flutter, are positively damped oscillations. Several recommendations are given for further experimental and theoretical studies.

1. Supercavitating hydrofoils--Ventilation--Flutter--Towing basin tests
2. Partially cavitating hydrofoils--Flutter--Towing basin tests
3. Supercavitating hydrofoils--Oscillation (Cavity-induced)--Water-tunnel tests
4. Partially cavitating hydrofoils--Oscillation (Cavity induced)--Water-tunnel tests

I. Besch, Peter K.

Naval Ship R&D Center. Report 3000.
FLUTTER AND CAVITY-INDUCED OSCILLATION OF A TWO-DEGREE-OF-FREEDOM HYDROFOIL IN TWO-DIMENSIONAL CAVITATING FLOW, by Peter K. Besch. Apr 1969. vii, 57p. illus., refs. UNCLASSIFIED

Two hydrofoil flutter tests were performed at the Naval Ship Research and Development Center using a two-degree-of-freedom, semiwedge hydrofoil in two-dimensional cavitating flow. In the first test, conducted in the high-speed towing basin, four distinct cavity lengths were tested. Flutter occurred for cavities 1/2 and several chords in length. Cavity-induced oscillations may have occurred for 1-chord cavities, but no oscillations were observed for 2-chord cavities. The flutter results are compared with flutter boundaries predicted by partially cavitating and supercavitating flutter theories. It is concluded that the experimental flutter results do not disagree with the predicted values.

In the second test, conducted in the 24-in. variable-pressure water tunnel, cavity lengths were varied from 0 to 3 chords. Cavity-induced oscillations were observed for cavities between 0.4 and 1.4 chords in length, but other cavity lengths were free of oscillation. The oscillations are discussed in terms of forced oscillations of a coupled two-degree-of-freedom elastic system. It is concluded that the cavity-induced oscillations, unlike flutter, are positively damped oscillations. Several recommendations are given for further experimental and theoretical studies.

1. Supercavitating hydrofoils--Ventilation--Flutter--Towing basin tests
2. Partially cavitating hydrofoils--Flutter--Towing basin tests
3. Supercavitating hydrofoils--Oscillation (Cavity-induced)--Water-tunnel tests
4. Partially cavitating hydrofoils--Oscillation (Cavity induced)--Water-tunnel tests

I. Besch, Peter K.